

MALDI plate and co-crystallized with α -cyano-4-hydroxycinnamic acid [27]. This plate was then loaded into the QSTAR Pulsar *i* (Applied Biosystems) at Hitachi Science Systems (Ibaraki, Japan).

Cloning of porcine epithelial cell adhesion molecules (Ep-CAM)

The porcine Ep-CAM gene was amplified from the mRNA of the small intestine by RT-PCR with mix primers (Sense: 5'-CDKCYAARTGYTTGGYGATG-3' Antisense: 5'-RMCACMACSACAATRACRGC-3') prepared based on the sequence data from humans [28], mice [29], and rats [30]. The 5' and 3' regions were analyzed with a GeneRacer kit (Invitrogen, Carlsbad, CA) by oligocapping and 3'RACE methods with primers prepared by the sequence data obtained from the internal porcine Ep-CAM (5' region: 5'-AGGTCCATCCTTTTGAATG-3', 5'-AGGTACCATTACTGCTTG-3', 3' region: 5'-ATTACCAACTGGATCCCAA-3', 5'-ATGAATCCTTGTTCCA-TTCC-3'). The sequencing was performed using the ABI3700 at Hitachi Science Systems (Tokyo, Japan).

Transfection of cells

Full-length porcine Ep-CAM was amplified by RT-PCR with primers (sense: 5'-ATTACTAATAGCTAGCATGGCGCCCCCAGGTCCT-3', antisense: 5'-AGCACTGAATTCCTTATGCATTGAGTTCCTAT-3', *NheI*, and *EcoRI* restriction enzyme site showed by underlining). It was then ligated into pIRES2-EGFP Vector (BD Biosciences Clontech, Palo Alto, CA) in front of the enhanced GFP (EGFP)-coding region at the *NheI* and *EcoRI* sites using the DNA Ligation Kit Ver.2 (Takara Biomedicals, Shiga, Japan) and sequenced. Because it contained the internal ribosome entry site (IRES), this plasmid (pIRES2-EGFP-pEp-CAM) was able to express both porcine Ep-CAM and EGFP. pIRES2-EGFP-pEp-CAM was transfected into COS-7 (ATCC, CRL-1651) in Opti-MEM (Invitrogen) by electrophoresis using Gene Pulser Xcell (Bio-Rad) [31]. After 48 h, the cells were stained first with 10 μ g/ml mAb (5-15-1) or an isotype control (mouse IgG2b, BD PharMingen), then with CY 5-conjugated anti-mouse IgG (Jackson, West Grove, PA) diluted 1:400, and finally analyzed by flow cytometry using FACSCalibur (Becton Dickinson).

Results

mAb (5-15-1) reacted with epithelium of porcine small intestine

First, isolated porcine IECs were injected into BALB/c mice to generate mAbs capable of recognizing a unique cell surface molecule of IECs. A total of 10 mAbs were generated and tested for their reactivity using frozen

sections prepared from porcine small intestine by immunohistochemical analysis. One of the mAbs, designated as mAb (5-15-1) with mouse IgG2b subclass, strongly reacted with the epithelium all the way from the villus (Fig. 1Aa) to the crypt (Fig. 1Ab) regions. Interestingly, the immunoreactivity was most strongly shown on the basolateral surface of the epithelium. An isotype control (Mouse IgG2b) did not react with the tissue sections of villus and crypt epithelium (Figs. 1Ac and d).

mAb (5-15-1) reacted with the 41–43 kDa protein of porcine small intestine when Western blot analysis was performed under nonreducing conditions

Inasmuch as 5-15-1 reacted with the epithelium of the porcine small intestine, the next logical step was to elucidate the molecular weight of the antigen recognized by 5-15-1. After immunoprecipitation of the small intestine with 5-15-1, a molecular mass of 41–43 kDa protein was detected by Western blot analysis under nonreducing conditions (Fig. 1Ba). Of course, this band was not detected in the negative control using the isotype control (mouse IgG2b) for immunoprecipitation or PBS instead of the lysate of the porcine small intestine (Fig. 1Ba). Nor was the band detected under reducing conditions (Fig. 1Bb). However, the band corresponding to the 5-15-1-specific antigen was detected by a G.P. Sensor, carbohydrate detection kit (Fig. 1Bc). These findings suggest that the surface antigen recognized by 5-15-1 belongs to a family of glycoproteins.

Immunoreactivity of mAb (5-15-1) with the other epithelial cells in mucosa-associated tissues

To further examine the immunoreactivity of 5-15-1 in several other mucosa-associated and systemic tissues, tissue sections were prepared from esophagus, stomach, duodenum, jejunum, ileum, appendix, colon, lung, spleen, and liver for immunohistological examination (Fig. 2). Among mucosa-associated epithelia, esophageal epithelial cells were stratified and flattened like skins cells and did not react with 5-15-1 (Fig. 2Aa). The lamina propria of the fundus ventriculi in the stomach is composed of fundic glands located under the epithelium and characterized by chief, parietal cells, and nebenzellen cells [32,33]. The newly developed mAb 5-15-1 reacted neither with the epithelial cells (Fig. 2Ab) nor with the chief, parietal, and nebenzellen cells in the fundic glands (Fig. 2Ac). When duodenum containing glandulae duodenales were examined, duodenum epithelial cells in the villus (Fig. 2Ad), crypt (Fig. 2Ae), and glands (Fig. 2Af) reacted with 5-15-1. The intestinal tract is composed of organized lymphoid structures known as gut-associated lymphoid tissue (GALT), an important inductive site for the mucosal immune system [2]. Therefore, sections of Peyer's patches (PPs) were examined for their reactivity with 5-15-1. Follicle-associated epithelium (FAE), one of the unique features of PPs,

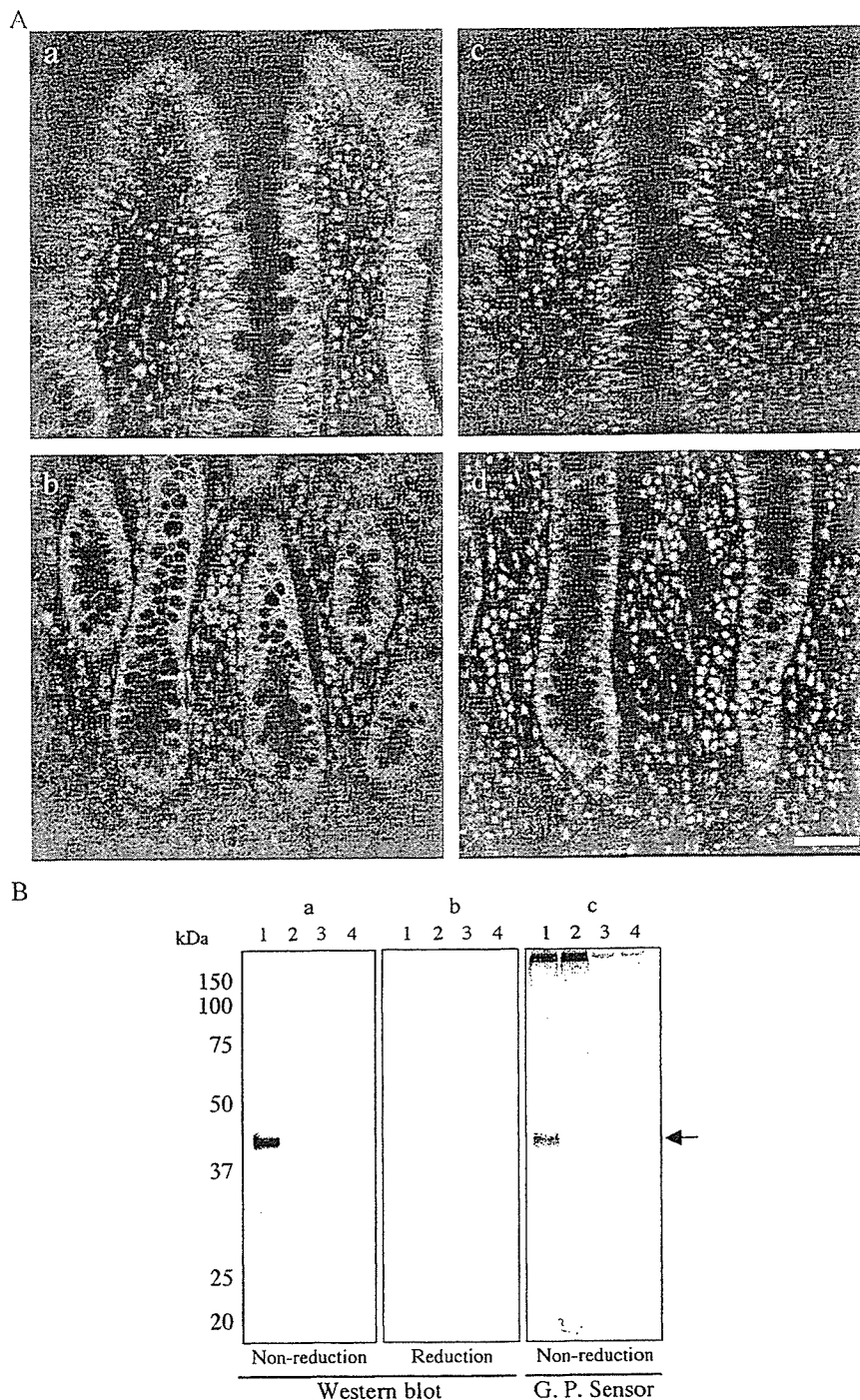


Fig. 1. Immunohistochemical and Western blot analyses of small intestine with mAb (5-15-1). Panel A shows tissue sections (5 μm) stained with the newly established mAb (5-15-1; mouse IgG2b) and with FITC-conjugated anti-mouse IgG followed by counterstaining with propidium iodate. (Aa and b) The immunoreactivity of 5-15-1; (Ac and d) the immunoreactivity of the isotype control. (Aa and c) The immunoreactivity in villus; (Ab and d) the immunoreactivity in the crypt. All of the intestinal epithelial cells (IECs) reacted with 5-15-1. Scale bar = 50 μm. Panel B shows the lysate of the small intestine (lanes 1 and 2) or the control (PBS, lanes 3 and 4), which was immunoprecipitated with 5-15-1 (lanes 1 and 3) or with an isotype control (mouse IgG2b, lanes 2 and 4) and then analyzed by Western blot. A protein measuring approximately 41–43 kDa was visible under nonreducing conditions (a) but not under reducing conditions (b). This 41–43 kDa protein was also detected under nonreducing conditions by G.P. Sensor (c).

exhibited strong immunoreactivity to 5-15-1 (Fig. 2Ag), while the leukocytes in PPs did not (Fig. 2Ah). Both the large (Fig. 2Ai) and the small (Figs. 1Aa and b) intestinal epithelium strongly reacted to 5-15-1, as did some alveolar cells and all of the epithelial cells of the bronchus in the lung

(Fig. 2Aj). However, neither hepatocytes (Fig. 2Ak) nor splenocytes (Fig. 2Al) showed reactivity to 5-15-1. Looked at collectively, these results suggest that 5-15-1 specifically reacted with mucosal epithelia composed of columnar epithelial cells.

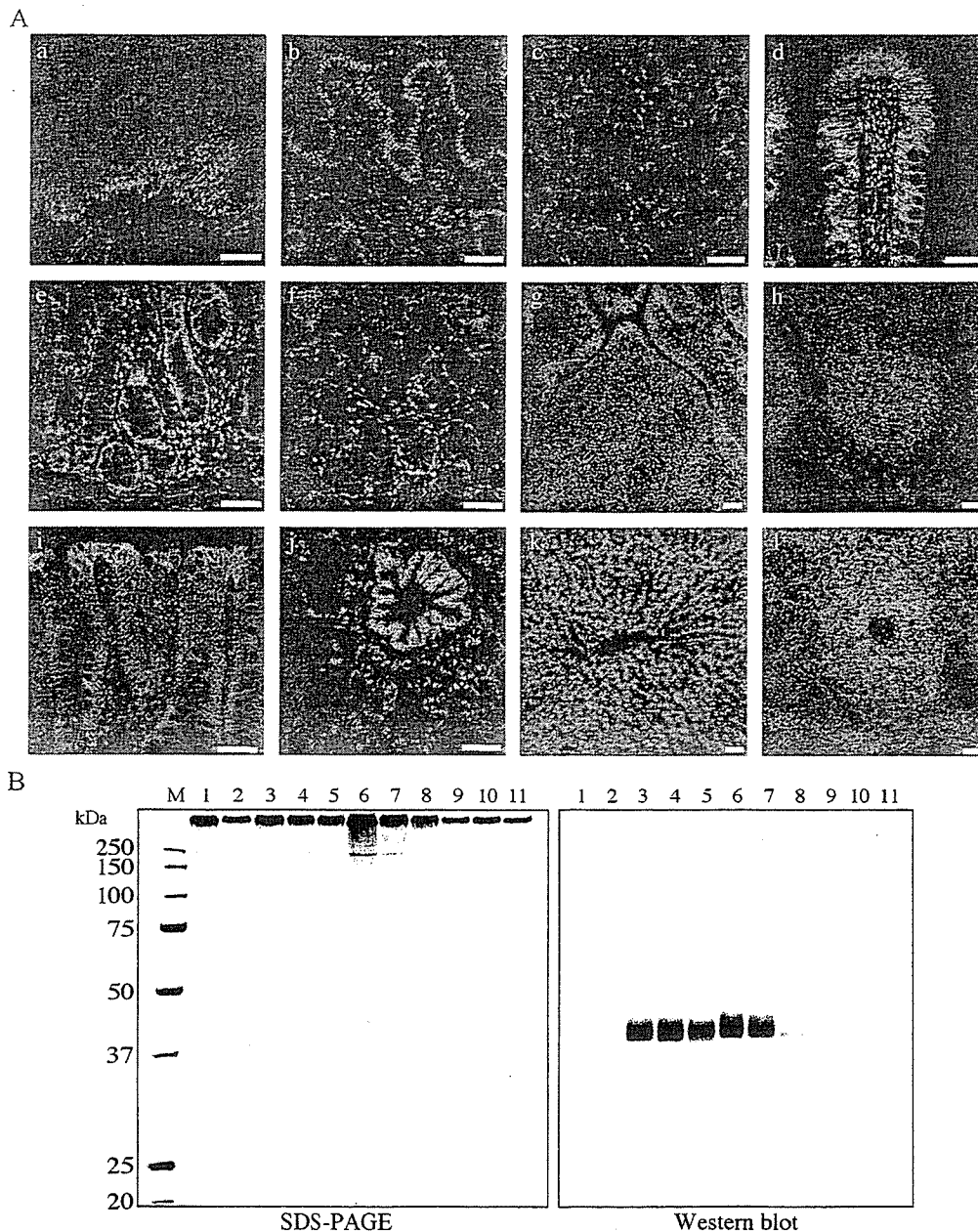


Fig. 2. Immunohistochemical and Western blot analyses of different mucosa-associated tissues with mAb (5-15-1). Panel A shows tissue sections (5 μ m) stained with 5-15-1 and FITC-conjugated anti-mouse IgG followed by counterstaining with propidium iodide. Almost all of the epithelial tissues, with the exception of the esophagus and stomach, reacted with 5-15-1. (a) Esophageal epithelium, (b) stomach epithelium, (c) fundic gland in stomach, (d) epithelium in duodenum, (e) crypt in duodenum, (f) gloandulae deodenaes in duodenum, (g) follicle-associated epithelium (FAE) in Peyer's patch, (h) lymphoid follicle in Peyer's patch, (i) epithelium in colon, (j) epithelium in lung, (k) hepatocyte in liver, (l) splenocyte in spleen. Scale bar = 50 μ m. Panel B shows the results obtained when lysates (5 mg) of different mucosa-associated tissues were immunoprecipitated with 5-15-1 (10 μ g/ml) and then analyzed by Western blot. The left panel shows the data obtained using SDS-PAGE, the right panel that obtained using Western blot. A protein with a molecular mass of 41–43 kDa was visible in the duodenum, jejunum, ileum, appendix, colon, and lung but not in the esophagus, stomach, liver, and spleen under nonreducing conditions. (1) Esophagus, (2) stomach, (3) duodenum, (4) jejunum, (5) ileum, (6) appendix, (7) colon, (8) lung, (9) liver, (10) spleen, (11) mAb alone.

Immunoprecipitation and Western blot analysis revealed the presence of the 41–43 kDa protein in all mucosa-associated tissues except the esophagus and stomach

We next used immunoprecipitation and Western blot analyses to confirm our immunohistochemical findings regarding the tissue specificity of 5-15-1 for several

mucosal-associated epithelia. Lysates prepared from different mucosa-associated and systemic tissues were precipitated with 5-15-1 and then analyzed by SDS-PAGE and Western blot analyses under nonreducing conditions. The antigen corresponding to a molecular mass of 41–43 kDa was detected in the duodenum, jejunum, ileum, appendix, colon, and lung, but not in the esophagus, stomach, spleen, and liver. The results obtained by SDS-PAGE and

Western blot analyses of these different tissue extracts (Fig. 2B) confirmed the data generated by the immunohistochemical analysis (Fig. 2A). Further, the data analyzed by Western blot revealed that the expression level of the antigen was roughly equal in the duodenum, jejunum, ileum, appendix, and colon, but considerably lower in the lung (Fig. 2B).

IELs but not splenocytes and PBMCs reacted with 5-15-1

Since 5-15-1 specifically reacted with the glycoprotein antigen (41–43 kDa) associated with the intestinal epithelium, we sought to determine whether a similar protein is also expressed by neighboring IELs. Flow cytometry was used to determine the immunoreactivity to 5-15-1 of IELs and IECs isolated from porcine small intestine. Splenocytes and PBMCs isolated from the same pig served as controls. First, IELs were separated from IECs on the basis of cell size and granularity (Fig. 3a). A fraction of IELs was greater than 98% positive for CD45, while the IECs fraction did not contain any CD45-positive cells (data not shown). As expected from the findings discussed above (Fig. 1A), freshly isolated IECs were positive for 5-15-1 (Fig. 3b). Interestingly, however, IELs also reacted with 5-15-1 (Fig. 3c). When the mean fluorescence intensity of the two fractions was compared, that of IELs was weaker than that of IECs (Fig. 3f). Splenocytes (Fig. 3d) and PBMCs (Fig. 3e) did not react with 5-15-1. These findings demonstrate that the glycoprotein, which reacted with 5-15-1, was also expressed by IELs in addition to IECs in the intestinal epithelium.

MALDI-TOF-MS and tandem MS analysis of 5-15-1 reactive 41–43 kDa protein resulted in the identification of a porcine homologue of the human pan-carcinoma antigen epithelial glycoprotein (EGP), or alias epithelial adhesion molecule (Ep-CAM)

Since it was expressed by both IECs and IELs, we sought to identify the exact nature of the 41–43 kDa protein recognized by 5-15-1. The antigen was first purified from small intestine lysates using affinity chromatography with 5-15-1 and then separated out using SDS-PAGE (Fig. 4A). When the 41–43 kDa protein was analyzed by MALDI-TOF-MS analysis after tryptic digestion, several major peaks were identified (Fig. 4B). Four major peaks (asterisks) were randomly selected and further analyzed by tandem MS. The amino acid sequence of one of the peaks (arrow in Fig. 4B) was identified as IADVAYFEK (Fig. 4C). A search of the “MASCOT” database confirmed this sequence as human pan-carcinoma antigen epithelial glycoprotein (EGP), or alias epithelial adhesion molecule (Ep-CAM). In contrast, the other three peaks were identified as actin (data not shown).

Cloning of porcine Ep-CAM

To formally prove that the antigen of 5-15-1 is a porcine homologue of human Ep-CAM, the next logical step was to clone and sequence the porcine Ep-CAM. Fig. 5 shows both the sequence including the initiation and stop codon and the predicted amino acid sequence.

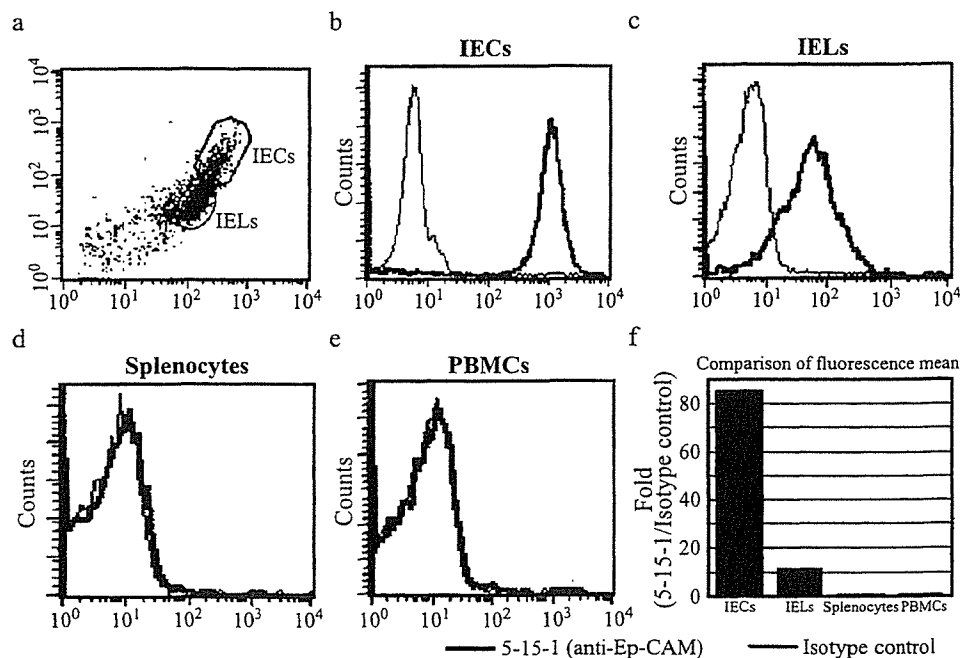


Fig. 3. Immunoreactivity of mAb (5-15-1) against IECs, IELs, splenocytes, and PBMCs. Isolated IECs, IELs, splenocytes, and PBMCs were stained with mAb (5-15-1) and FITC-conjugated anti-mouse IgG and then analyzed using flow cytometry. IECs and IELs were separated based on cell size and granularity (a). IECs (b) and IELs (c), but not splenocytes (d), and PBMCs (e) reacted with 5-15-1. The fluorescence mean intensity was also examined (f).

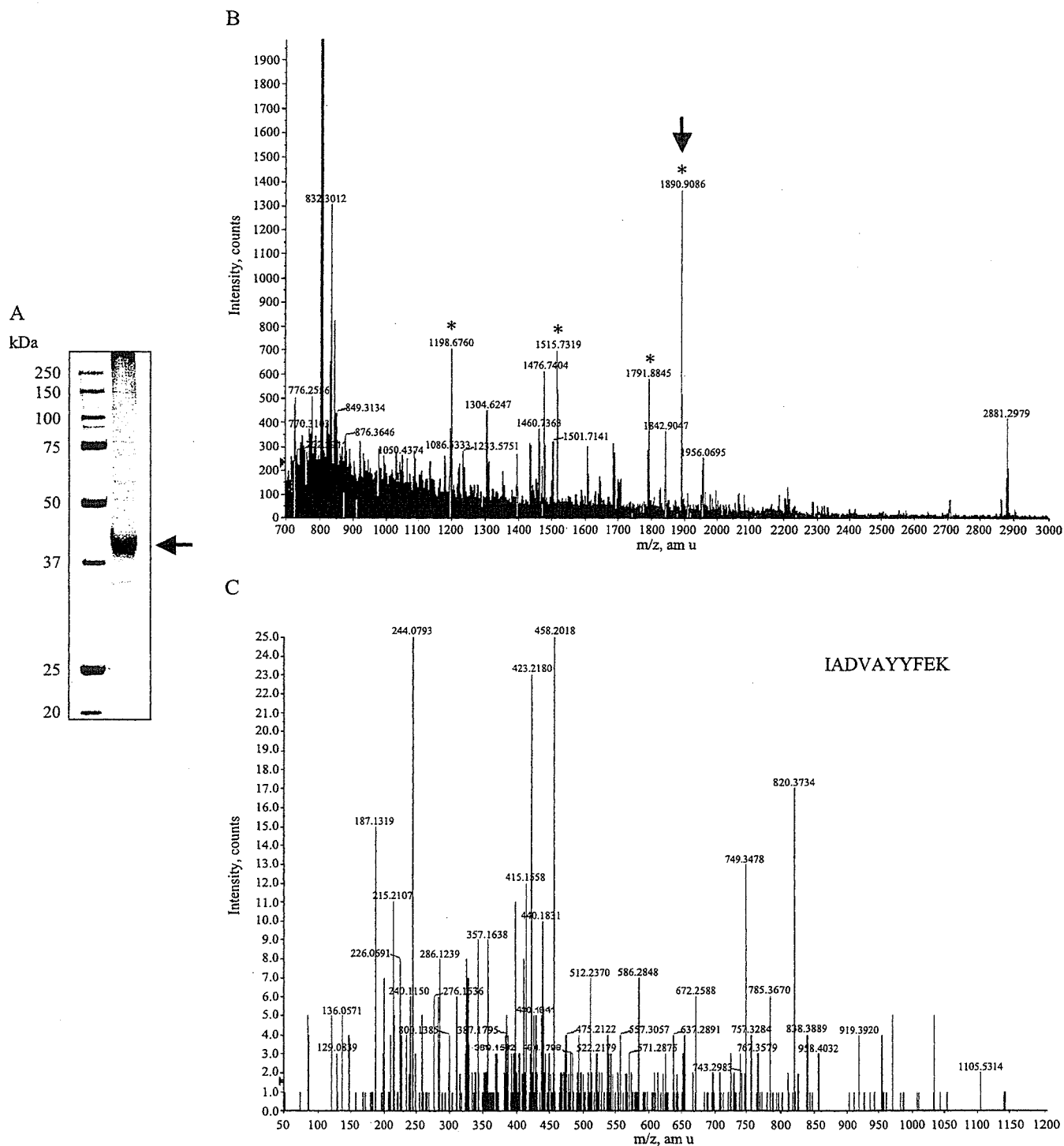


Fig. 4. Identification of the antigen purified by affinity chromatography with 5-15-1. Panel A shows the SDS-PAGE analysis of the antigen purified by affinity chromatography with 5-15-1. A protein with a molecular mass of 41–43 kDa was analyzed by MALDI-TOF-MS and tandem MS analysis. Panel B shows the MALDI-TOF-MS spectrum of the 41–43 kDa antigen digested by trypsin. Four major peaks (asterisks) were further analyzed by tandem MS. Panel C shows that the tandem MS spectrum of one of the four peaks (arrow in Panel B) was sequenced and identified as “IADVAYYFEK.”

As one might expect, the cloned sequence contains tandem MS-identified “IADVAYYFEK.” The sequence data were then registered with GenBank (Accession number: AB161197). The cDNA contains an open reading frame (ORF) of 945 bp and encodes for 314 amino acids. Compared with human, mouse, and rat sequences, the

porcine Ep-CAM displays 82.9%, 71.3%, and 71.8% homology at the nucleotide level and 82.8%, 78.1%, and 76.8% homology at the amino acid level, respectively (Fig. 5). Porcine Ep-CAM is a type-I transmembrane protein of which the first 23 amino acids are putatively the signal sequence. A 242 amino acid, cystein-rich extracellular

```

GAAAGCCCGCGCACC 15
ATGGCGCCCCCAGGTCTCGCGTTCGGGCTCCTGCTCGCCGCGGCGACGGCGCGGTG 75
1  M A P P Q V L A F G L L L A A A T A A V
GCCGCGCCCAACAGGATGTGTGTGAAAACACAACTGACCACAACTGCTCTTTG 135
21  A A A Q Q G (C) V (C) E N Y K L T T N (C) S L
AATGCGCTTGGTCAGTGCCAGTGTACTTCAATGGTGCACAAAATCTGTCTTTGCTCA 195
41  N A L G Q (C) Q (C) T S I G A Q N S V I (C) S
AAATTGGCTTCCAAATGTTTGGTGAAGGCAGAAATGACTGGGTCAAAGGATGGGAGA 255
61  K L A S K (C) L V M K A E M T G S K A G R
AGACTGAAACCAGAGAATGCTATCCAGAACACGATGGGCTCTATGATCCTGACTGTGAC 315
81  R L A K P E N A I Q N N D G L Y D P D (C) D
GAGAATGGGCTCTTCAAAGCCAAGCAGTGTAAATGGTACCTCCATGTGCTGGTGTGAAC 375
101 E N G L F K A K Q (C) N G T S M (C) W (C) V N
ACTGCTGGGTCAGAAAGGACCGATAAGGACTCTGAAATATCCTGTTGGAGCGAGTGAGG 435
121 T A G V R R T D K D S E I S (C) L E R V R
ACCTATGGATCATCATGAACATAAACACAAAACAAGAGAAAACCTTATGATGCACACA 495
141 T Y W I I I E L K H K T R E K P Y D V T
AGTTTGAGAATGCACTCAAGGAGGTAATCACGGATCGTTACCAACTGGATCCCAATAT 555
161 S L Q N A L K E V I T D R Y Q L D P K Y
ATTACAAATATTCTGTATGAGAATGATATTATCACCATTGATCTGGTACAAAATCTTCT 615
181 I T N I L Y E N D I I T I D L V Q N S S
CAGAAAACCTGAATGAAGTAGACATAGCTGATGTAGCTTATTATTTTGAAGAGATGTT 675
201 Q K T L N E V D I A D V A Y Y F E K D V
AAAGATGAATCCTTGTCCATCCAAAAGGATGGACCTGAGAGTAAATGGGAACACTAG 735
221 K D E S L F H S K R M D L R V N G E L L
GATCTGGATCCTGGTCAAACCTCAATTTACTATGTTGATGAAAACCCACTGAATTTTCA 795
241 D L D P G Q T S I Y Y V D E K P P E F S
ATGCAGGGTCTACAGGCTGGTATTATGCTGTCATTGCAGTTGTGGCGATAGCAATTTGTT 855
261 M Q G L Q A G I I A V I A V V A I A I V
GCTGGCATCATTGTGCTGATTGTTTCCACGAAGAAAAGAAGGGCAAAGTATGAGAAGCT 915
281 A G I I V L I V S T K K R R A K Y E K A
GAGATAAAGGAGATGGGCGAGATGCATAGGGAACCTCAATGCATAACACCGTAATTTGAGG 975
301 E I K E M G E M H R E L N A * 314
GGTAACTACAAGAAGGGAAATTAGCACAGGCTCAGATTACTAATGTGTGGGCAAGAGA 1035
AGATCTTTGAGGACCACTATTGTGTAGTTAACATCGTATGTTGTGATAGTTAAACCTG 1095
CATTAAAATAGAAGCAGCTTGAATTTGACTTTACTAATCTAAAATTTGACCACAGATG 1155
TCATAAGTATGCAGATTTGATATTAACCCAGCATTGGACTGCATAGTTTGAATTTATTT 1215
ATGCCTAGCATTGAAAGGTATGCATTAAATATGCTTCCACAGTAGAGTCTGAATGACTAC 1275
TGTCTTACCCATTTGTATTAATGTTTGCCTTCTGTTTACTTTGAGTCTTGTACATAT 1335
AAACTTTTTTATGAACTACAAAATAAACATTTAAAAATGAAAAAATAAAAAAAAAAAAA 1395

```

Fig. 5. DNA and amino acid sequence of porcine Ep-CAM. An open reading frame predicts a protein of 314 amino acids. A putative signal sequence (first bolded underline), 12 cysteine residues (circles), two potential N-linked glycosylation sites (bold and dotted underline), and one transmembrane domain (dotted underline) are indicated. The amino acid sequence matched that of the molecule identified by MALDI-TOF-MS and tandem MS analyses was shown in the box.

domain is followed by a 23 amino acid hydrophobic transmembrane domain and a 26 amino acid highly charged intracellular domain. There are two potential N-linked glycosylation sites in the extracellular domain. These molecular characteristics are very similar to those seen in human, mouse, and rat Ep-CAM [28–30].

mAb (5-15-1) reacted COS-7 transfected with the cDNA of porcine Ep-CAM

To directly confirm that the antigen of 5-15-1 is porcine Ep-CAM, we generated COS-7 cells transfected with the cDNA of porcine Ep-CAM. For the transfection, we purposely used the pIRES2-EGFP vector system since it is capable, by merit of its containing the IRES sequence, of expressing enhanced GFP (EGFP) and porcine Ep-CAM under one mRNA transcript [34]. The expression plasmid map (pIRES2-EGFP-pEp-CAM) is shown in Fig. 6A. When successfully transfected with pIRES2-EGFP-pEp-CAM, COS-7 cells expressed EGFP and Ep-CAM that could be recognized by 5-15-1 (Fig. 6B). In contrast,

COS-7 transfected with an empty vector (pIRES2-EGFP) expressed EGFP but did not react with 5-15-1. These findings demonstrate that 5-15-1 possesses specificity for porcine Ep-CAM.

Expression of Ep-CAM by both IECs and IELs

To definitively prove that Ep-CAM is expressed by both the IECs and IELs of the intestinal epithelium, we performed an immunohistochemical analysis of the intestinal epithelium using FITC-conjugated 5-15-1 specific for Ep-CAM and rhodamine-coupled anti-porcine CD45 mAb together with DAPI counterstaining. The immunohistochemical analysis revealed that Ep-CAM was expressed by IECs and IELs. It is important to note that the expression of Ep-CAM and CD45 were colocalized on the cell surface of IELs (arrowhead in Fig. 7A). In contrast, CD45-positive lymphocytes located in the lamina propria region did not express Ep-CAM (arrow in Fig. 7A). CD45-positive splenocytes also did not react with Ep-CAM-specific mAb 5-15-1 (Fig. 7B). These findings

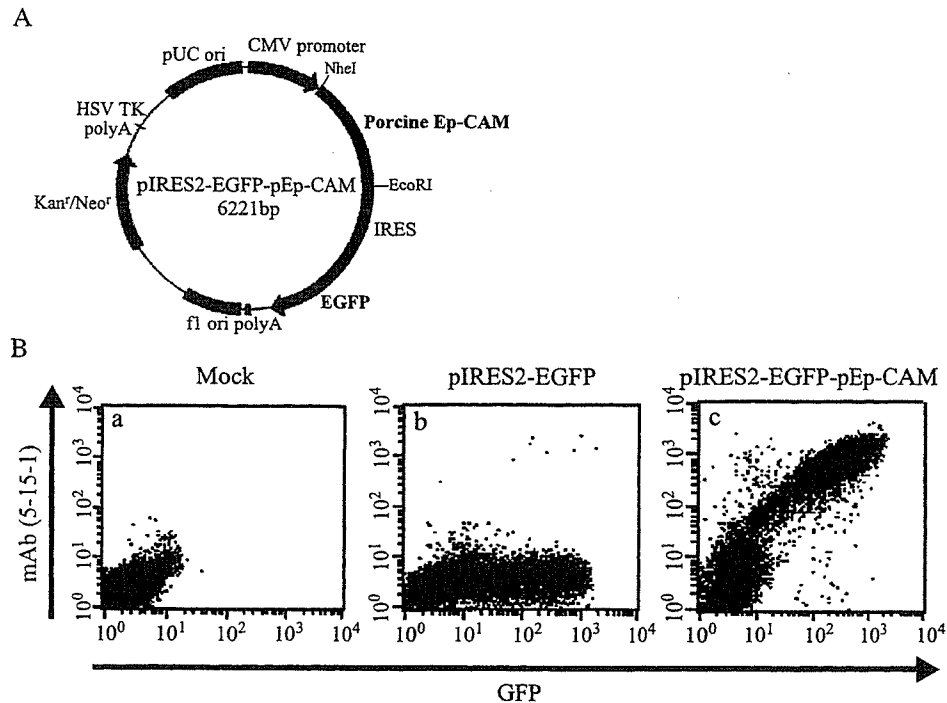


Fig. 6. Ep-CAM-specific 5-15-1 possessed specificity against COS-7 transfected with the cDNA of porcine Ep-CAM. Panel A shows the structure of the porcine Ep-CAM expression plasmid (pIRES2-EGFP-pEp-CAM). This plasmid (pIRES2-EGFP-pEp-CAM) is used for the expression of both porcine Ep-CAM and enhanced GFP (EGFP) because it contains the internal ribosome entry site (IRES). Panel B shows the flow cytometric analysis of nontransfected COS-7 (a), COS-7 transfected with empty vector (pIRES2-EGFP) (b), and pIRES2-EGFP-pEp-CAM (c) by using mAb (5-15-1). mAb (5-15-1) reacted only with COS-7 transfected with pIRES2-EGFP-pEp-CAM (c).

formally demonstrate that Ep-CAM is expressed by both IECs and CD45-positive IELs.

Discussion

The mucosal immune system has been shown to possess several biological characteristics that distinguish it from the systemic immune system [2]. For example, a sheet of intestinal epithelium provides a physical and immunological barrier against invading pathogens by forming an interdependent mucosal transect between IECs and IELs. One IEL is usually surrounded by six to eight IECs [2]. When $\gamma\delta$ T cells representing approximately 50% of the murine IELs were removed, epithelial cell growth and MHC class II expression deteriorated [35]. This mutually beneficial relationship between IECs and IELs is reciprocally regulated by a group of mucosal cytokines including IL-7, IL-15, and SCF [17–19]. However, the physical and biological retention mechanism, which maintains IELs in the cellular pocket created by IECs in the intestinal epithelium, still remains unknown. To shed light on this issue, we sought to identify the novel molecule that helps retain IECs and IELs by generating a panel of mAbs specific for the intestinal epithelium. To identify the molecule on the cell surface that allows for physical cross-talk between IECs and IELs, we generated mAbs strongly reactive for the porcine epithelium by immunizing

isolated and purified porcine IECs. After splenocytes isolated from immunized Balb/c mice were fused with myeloma (Sp2/0-Ag14), a total of 10 mAb-producing hybridomas were originally generated and screened for their specificity against isolated cells from the porcine intestine using flow cytometry (data not shown). Among these hybridomas, one, designated mAb 5-15-1, was found to strongly react with the basolateral surface of the intestinal epithelium (Fig. 1A). After immunoprecipitation, the antigen of 5-15-1 was detected at a molecular mass of 41–43 kDa by Western blot analysis under nonreducing conditions (Fig. 1B). Furthermore, the antigen was also characterized by using a G.P. Sensor, carbohydrate detection kit (Fig. 1B). Taken together, these data suggest that the surface antigen recognized by mAb 5-15-1 belongs to a family of membrane glycoproteins.

In order to identify the specific antigen of 5-15-1, we next attempted to purify the corresponding molecule from the lysate of the porcine small intestine using affinity chromatography with 5-15-1 (Fig. 4A). When the four major peaks identified by the MALDI-TOF-MS analysis of the purified trypsin-digested antigen (Fig. 4B) were further characterized by tandem MS, one peak was found to match with the peptide sequence of IADVAYYFEK, which corresponds to the human pan-carcinoma antigen epithelial glycoprotein (EGP). EGP was originally identified when various mAbs (e.g., MH99, AUA1, MOC31, 323/A3, KS1/4, GA733, HEA125) were developed and used for the

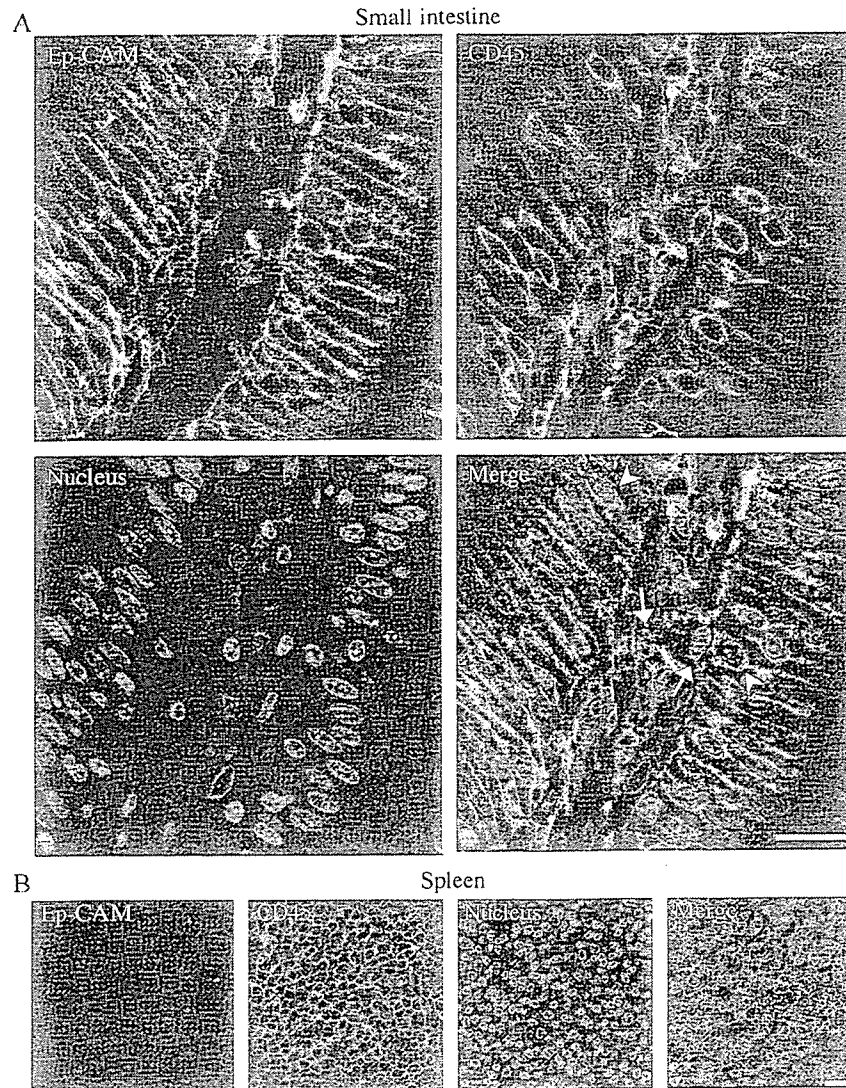


Fig. 7. Double immunohistochemical analysis of porcine small intestine and spleen with mAb 5-15-1 (anti-porcine Ep-CAM) and anti-porcine CD45 mAb. Tissue sections (5 μ m) were incubated with anti-porcine Ep-CAM (5-15-1) and anti-porcine CD45 and then stained with FITC-conjugated anti-mouse IgG2b and rhodamine-conjugated anti-mouse IgG1, respectively. The slides were then counterstained by DAPI. In the small intestine, CD45-positive IELs (arrowhead) were costained with anti-porcine Ep-CAM (5-15-1), but such colocalization was not seen for lamina propria lymphocytes (LPLs, arrow) (A). Further, CD45-positive splenocytes did not react with anti-porcine Ep-CAM (5-15-1) (B). Scale bar = 20 μ m.

analysis of human epithelial carcinoma [36–41]. Since EGP was initially shown to be expressed by human epithelial carcinoma, the molecule has become the target of EGP-specific immunotherapy and gene therapy strategies [42,43]. However, because EGP is an epithelial differentiation antigen but not a tumor-specific antigen, anti-EGP therapy can cause severe side effects [44]. A few years ago, EGP was shown to be capable of functioning as a Ca^{2+} -independent homophilic cell-to-cell adhesion molecule and received the new designation of epithelial cell adhesion molecule (Ep-CAM) [45,46]. Our present findings further demonstrate the physical homophilic cell-to-cell adhesion capability of Ep-CAM for the formation and maintenance of a sheet-like structure of intestinal epithelium. Thus, E-cadherin was shown to play a crucial role in the maintenance of the intestinal epithelium structure [47]. Ep-CAM may

also play a physical role in sustaining the IELs population in the intestinal epithelium since IELs also possess specificity against 5-15-1 (Figs. 3 and 7). Thus, intestinal Ep-CAM is considered to be a key physical retention molecule for IECs and IELs and may provide a first line of defense against mucosal infection. It was recently reported that E-cadherin was recognized as the ligand molecule of internalin expressed by *Listeria monocytogenes* for their invasion to the host [48]. Although we still do not know exact molecular mechanism for the intercellular bacterial entry, Ep-CAM might be target molecule for several microorganisms to enter the host via the destruction of mucosal epithelium created by IECs and IELs.

Only one of the peaks exhibited the peptide sequence of IADVAYYFEK, which corresponds to Ep-CAM (Fig. 4); the other three peaks identified by MALDI-TOF-MS

analysis were matched with the peptide sequence of actin by the subsequent tandem MS analysis (data not shown). Although the reactivity of 5-15-1 was only confirmed in mucosa-associated epithelium (Figs. 1 and 2), it is well known that anti-actin mAb generally reacts with most eukaryotic cells. Thus, actin is the major protein expressed by all of the mammalian tissues. When we performed the immunohistochemical staining for small intestinal epithelium using 5-15-1 and anti-actin mAb, epithelial cells reacted with both mAbs, as expected (data not shown). A previous study had reported that the cytoplasmic tail of Ep-CAM is capable of associating with the α -actinin [49]. This finding suggests the possibility of a biological association between Ep-CAM and the actin-based cytoskeleton in intestinal epithelial cells. This molecular interaction between the cytoplasmic tail of Ep-CAM and α -actinin has been considered to be a key component of the homophilic adhesion mechanism [49]. These findings lend further credibility to the possibility that the Ep-CAM expressed by both IECs and IELs may behave as a homophilic physical retention molecule for the heterologous cell-to-cell interaction in the intestinal epithelium.

To firmly confirm that 5-15-1 reacted specifically with porcine Ep-CAM, we cloned and sequenced porcine Ep-CAM and then examined the reactivity of 5-15-1 to COS-7 transfected with the isolated cDNA of porcine Ep-CAM (Fig. 6). The cloned cDNA contains an open reading frame (ORF) of 945 bp and encodes for 314 amino acids (Fig. 5). Compared to human, mouse, and rat sequences, the cloned porcine Ep-CAM displayed 71–83% and 77–83% homology at the nucleotide and amino acid levels, respectively (Fig. 5). Based on the characterization and comparison of the sequence with the known Ep-CAM in other species, the cloned porcine Ep-CAM was determined to be a type I transmembrane molecule with 12 conserved cystein residues and at least two N-glycosylation sites, like human, mouse, and rat Ep-CAM. Furthermore, the extracellular domain of porcine Ep-CAM also contained two epidermal growth factor (EGF)-like repeat motifs of CX₁CX₈CX₇CX₁CX₁₀C (position 27–59, EGF-I) and CX₃₂CX₁₀CX₅CX₁CX₁₆C (position 66–135, EGF-II), followed by a cysteine-poor domain (Fig. 5). The Ep-CAM polypeptide was originally shown to consist of 314 amino acids, including a 23 amino acid leader sequence, a 242 amino acid extracellular domain with two EGF-like repeats (EGF-I and EGF-II) within the cysteine-rich N-terminal part, a 23 amino acid transmembrane domain, and a 26 amino acid cytoplasmic domain [50]. Among these different sections of the polypeptide, the EGF repeats of the extracellular domain of the Ep-CAM molecule are the most immunodominant epitopes expressed on the cell surface [50,51]. Thus, the focus has been on generating mAbs specific for the EGF-I and -II portion of the Ep-CAM in different species [50,51]. The majority of the currently existing mAbs possess specificity for the first EGF repeat. Based on the Western blot analysis (Fig. 1B), Ep-CAM was detected under nonreducing but not under

reducing conditions. These findings suggest that 5-15-1 also recognized the cysteine-rich domain of Ep-CAM (e.g., EGF-1, EGF-2). The 5-15-1 specifically reacted with COS-7 cells that had been transfected with the expression plasmid containing the cloned cDNA of porcine Ep-CAM (pIRES2-EGFP-pEp-CAM), but not with the cells transfected with the empty plasmid of pIRES2-EGFP (Fig. 6). Collectively, these results confirm that, by using the newly developed mAb 5-15-1, we have identified the porcine counterpart of Ep-CAM both at the level of the cloned gene and the protein.

It was interesting to note that the expression of 5-15-1 reactive Ep-CAM seemed always to be associated with the presence of IELs in the mucosal epithelium. When 5-15-1 was reacted with several other mucosal tissue-associated epithelial cells in addition to the small intestine (Fig. 2A), epithelial cells in the esophagus and stomach did not react with 5-15-1, while the other mucosa-associated epithelium did and at rates similar to those seen for the small intestinal epithelium. Further, the spleen and liver did not react with 5-15-1. Interestingly, because the esophageal and stomach epithelia are known not to contain IELs [52], they would have no need to express Ep-CAM as the retention molecule between IECs and IELs. Immunoprecipitation and Western blot analysis were used to confirm that all mucosa-associated tissues with the exception of the esophagus and stomach react with 5-15-1 (Fig. 2B). These findings suggest that Ep-CAM is strongly expressed by the mucosal epithelia that are covered by columnar epithelial cells. Since the stomach epithelium has been shown to possess physiological and immunological characteristics that distinguish it from the other mucosa-associated epithelia, its expression of Ep-CAM could be different as well. Taken together with the previous data [41], our current findings suggest that Ep-CAM plays a key role in the physical retention of IECs and IELs in the intestinal epithelium.

Moreover, we used flow cytometry with the appropriate fluorescence-conjugated 5-15-1 to show that Ep-CAM was expressed by IELs but not by splenocytes and PBMCs (Fig. 3). Further, the immunohistochemical analysis indicated that Ep-CAM and CD45 were colocalized on the cell surface of IELs but not of lamina propria lymphocytes (LPLs) (Fig. 7A). These findings further support our contention that a homophilic adhesion molecule of Ep-CAM plays a major biological role in the physical interaction between IECs and IELs. Previous studies reported that $\alpha_E\beta_7$ integrin mediates T cell adhesion to epithelial cells through its binding to E-cadherin, a member of the cadherin family of adhesion molecules that is expressed selectively on epithelial cells [53–55]. In fact, IELs decreased in number but did not disappear in α_E integrin-deficient mice [56]. These data suggest the interesting possibility that another adhesion mechanism mediated by Ep-CAM contributes to the formation and maintenance of an intact intestinal epithelium by physically retaining IELs in the cellular pocket created by IECs and may create an environment of mucosal intranet for

the maintenance of immunological homeostasis. In support of this possibility, a previous study reported that Ep-CAM was expressed in murine thymocyte and might contribute to adhesive interactions between thymocytes and thymus epithelial cells [57]. Currently, we are attempting to directly determine the physical adhesion mechanism via Ep-CAM between IECs and IELs by the creation of Ep-CAM-deficient mice.

In summary, we have used the newly generated mAb 5-15-1 to identify Ep-CAM expression by both intestinal intraepithelial lymphocytes and intestinal epithelial cells. The cell surface antigen recognized by 5-15-1 was a glycoprotein of Ep-CAM with a molecular mass of 41–43 kDa. The characterization of 5-15-1 affinity chromatography-purified glycoprotein by the use of MALDI-TOF-MS and tandem MS analyses demonstrated that the antigen was the porcine homologue of the human pan-carcinoma antigen epithelial glycoprotein, known as alias Ep-CAM. The cloning of the 5-15-1 reactive glycoprotein further confirmed the identification of Ep-CAM at the nucleotide and amino acid levels. The specificity of 5-15-1 was formally proved using COS-7 cells transfected with the cDNA of the cloned porcine Ep-CAM. Interestingly, not only IECs but also IELs reacted with 5-15-1. Since our data demonstrate that both IECs and IELs express homophilic adhesion molecules of Ep-CAM, it is plausible that Ep-CAM is an important element of the physical retention network responsible for retaining IECs and IELs in the intestinal epithelium for the generation of innate defense system.

Acknowledgments

This work was supported by grants from CREST, JST, the Ministry of Education, Science, Sports and Cultures, the Ministry of Health and Welfare, and the Health Science Foundation, Japan.

We thank Mr. H. Fujita of Tokyo Shibaura Zouki and Dr. Nakura and his colleagues of Chugai Research Institute for Medical Science for their helpful sampling of the porcine tissues. We thank Mr. S. Watanabe and Ms. T. Kayamori of Hitachi Science Systems for their help in performing the molecular analyses using MALDI-TOF-MS and tandem MS. We also thank Dr. Kimberly McGhee for reading and editing the manuscript.

References

- [1] B. Creamer, The turnover of the epithelium of the small intestine, *Br. Med. Bull.* 23 (1967) 226–230.
- [2] J. Mestecky, R.S. Blumberg, H. Kiyono, J.R. McGhee, The mucosal immune system, in: W.E. Paul (Ed.), *Fundamental Immunology*, fifth ed., Lipponcott Williams & Wilkins, 2003, pp. 965–1020.
- [3] M. Furuse, T. Hirase, M. Itoh, A. Nagafuchi, S. Yonemura, S. Tsukita, Occludin: a novel integral membrane protein localizing at tight junctions, *J. Cell Biol.* 123 (1993) 1777–1788.
- [4] M. Furuse, K. Fujita, T. Hiiiragi, K. Fujimoto, S. Tsukita, Claudin-1 and -2: novel integral membrane proteins localizing at tight junctions with no sequence similarity to occludin, *J. Cell Biol.* 141 (1998) 1539–1550.
- [5] K. Morita, M. Furuse, K. Fujimoto, S. Tsukita, Claudin multigene family encoding four-transmembrane domain protein components of tight junction strands, *Proc. Natl. Acad. Sci. U. S. A.* 96 (1999) 511–516.
- [6] J.M. Anderson, C.M. Van Itallie, Tight junctions and the molecular basis for regulation of paracellular permeability, *Am. J. Physiol.* 269 (1995) G467–G475.
- [7] E.E. Schneeberger, R.D. Lynch, Structure, function, and regulation of cellular tight junctions, *Am. J. Physiol.* 262 (1992) L647–L661.
- [8] S. Tsukita, M. Furuse, M. Itoh, Multifunctional strands in tight junctions, *Nat. Rev., Mol. Cell Biol.* 2 (2001) 285–293.
- [9] M. Takeichi, Cadherin cell adhesion receptors as a morphogenetic regulator, *Science* 251 (1991) 1451–1455.
- [10] L. Shapiro, A.M. Fannon, P.D. Kwong, A. Thompson, M.S. Lehmann, G. Grubel, J.F. Legrand, J. Als-Nielsen, D.R. Colman, W.A. Hendrickson, Structural basis of cell–cell adhesion by cadherins, *Nature* 374 (1995) 306–307.
- [11] R. Kemler, From cadherins to catenins: cytoplasmic protein interactions and regulation of cell adhesion, *Trends Genet.* 9 (1993) 317–321.
- [12] T. Kucharzik, S.V. Walsh, J. Chen, C.A. Parkos, A. Nusrat, Neutrophil transmigration in inflammatory bowel disease is associated with differential expression of epithelial intercellular junction proteins, *Am. J. Pathol.* 159 (2001) 2001–2009.
- [13] D. Guy-Grand, M. Malassis-Seris, C. Briottet, P. Vassalli, Cytotoxic differentiation of mouse gut thymodependent and independent intraepithelial T lymphocytes is induced locally, *J. Exp. Med.* 173 (1991) 1549–1552.
- [14] A. Hayday, E. Theodoridis, E. Ramsburg, J. Shires, Intraepithelial lymphocytes: exploring the third way in immunology, *Nat. Immunol.* 2 (2001) 997–1003.
- [15] K. Suzuki, T. Oida, H. Hamada, O. Hitotsumatsu, M. Watanabe, T. Hibi, H. Yamamoto, E. Kubota, S. Kaminogawa, H. Ishikawa, Gut cryptpatches: direct evidence of extrathymic anatomical sites for intestinal T lymphopoiesis, *Immunity* 13 (2000) 691–702.
- [16] X. Cao, E.W. Shores, J. Hu-Li, M.R. Anver, B.L. Kelsall, S.M. Russell, J. Drago, M. Noguchi, A. Grinberg, E.T. Bloom, W.E. Paul, S.I. Katz, P.E. Love, W.J. Lenard, Defective lymphoid development in mice lacking expression of the common cytokine receptor gamma chain, *Immunity* 2 (1995) 223–238.
- [17] M. Yamamoto, H. Kiyono, Role of $\gamma\delta$ T cells in mucosal intranet, *Allergol. Intern.* 48 (1999) 1–5.
- [18] K. Inagaki-Ohara, H. Nishimura, A. Mitani, Y. Yoshikai, Interleukin-15 preferentially promotes the growth of intestinal intraepithelial lymphocytes bearing $\gamma\delta$ T cell receptor, *Eur. J. Immunol.* 27 (1997) 2885–2891.
- [19] L. Puddington, S. Olson, L. Lefrancois, Interactions between stem cell factor and c-Kit are required for intestinal immune system homeostasis, *Immunity* 1 (1994) 733–739.
- [20] K. Fujihashi, J.R. McGhee, M. Yamamoto, J.J. Peschon, H. Kiyono, An interleukin-7 Internet for intestinal intraepithelial T cell development: knockout of ligand or receptor reveal differences in the immunodeficient state, *Eur. J. Immunol.* 27 (1997) 2133–2138.
- [21] K. Fujihashi, S. Kawabata, T. Hiroi, M. Yamamoto, J.R. McGhee, S. Nisikawa, H. Kiyono, Interleukin 2 (IL-2) and interleukin 7 (IL-7) reciprocally induce IL-7 and IL-2 receptors on gamma delta T-cell receptor-positive intraepithelial lymphocytes, *Proc. Natl. Acad. Sci. U. S. A.* 93 (1996) 3613–3618.
- [22] T. Waldmann, Y. Tagaya, The multifaceted regulation of interleukin-15 expression and the role of this cytokine in NK cell differentiation and host response to intracellular pathogens, *Annu. Rev. Immunol.* 17 (1999) 19–49.
- [23] K. Hirose, H. Suzuki, H. Nishimura, A. Mitani, J. Washizu, T. Matsuguchi, Y. Yoshikai, Interleukin-15 may be responsible for early

- activation of intestinal intraepithelial lymphocytes after oral infection with *Listeria monocytogenes* in rats, *Infect. Immun.* 66 (1998) 5677–5683.
- [24] N. Ohta, T. Hiroi, M.-N. Kweon, N. Kinoshita, M.-H. Jang, T. Mashimo, J. Miyazaki, H. Kiyono, IL-15-dependent activation-induced cell death-resistant Th1 type CD8 $\alpha\beta$ ⁺NK1.1⁺ T cells for the development of small intestinal inflammation, *J. Immunol.* 169 (2002) 460–468.
- [25] M. Watanabe, Y. Ueno, T. Yajima, S. Okamoto, T. Hayashi, M. Yamazaki, Y. Iwao, H. Ishii, S. Habu, M. Uehira, H. Nishimoto, H. Ishikawa, J. Hata, T. Hibi, Interleukin 7 transgenic mice develop chronic colitis with decreased interleukin 7 protein accumulation in the colonic mucosa, *J. Exp. Med.* 187 (1998) 389–402.
- [26] M. Yamamoto, K. Fujihashi, K. Kawabata, J.R. McGhee, H. Kiyono, A mucosal intranet: intestinal epithelial cells down-regulate intraepithelial, but not peripheral, T lymphocytes, *J. Immunol.* 160 (1998) 2188–2196.
- [27] M. Yanagida, Y. Miura, K. Yagasaki, M. Taoka, T. Isobe, N. Takahashi, Matrix assisted laser desorption/ionization-time of flight-mass spectrometry analysis of proteins detected by anti-phosphotyrosine antibody on two-dimensional-gels of fibroblast cell lysates after tumor necrosis factor- α stimulation, *Electrophoresis* 21 (2000) 1890–1898.
- [28] B. Simon, D.K. Podolsky, G. Moldenhauer, K.J. Issebacher, S. Gattoni-celli, S.J. Brand, Epithelial glycoprotein is a member of family of epithelial cell surface antigens homologous to nidogen, a matrix adhesion protein, *Proc. Natl. Acad. Sci. U. S. A.* 87 (1990) 2755–2759.
- [29] P.L. Bergsagel, C. Victro-Kobrin, C.R. Timblin, L. Trepel, W.M. Kuehl, A murine cDNA encodes a pan-epithelial glycoprotein that is also expressed on plasma cells, *J. Immunol.* 148 (1992) 590–596.
- [30] J. Wurfel, M. Rosel, S. Seiter, C. Claas, M. Herlevsen, R. Weth, M. Zoller, Metastasis-association of the rat ortholog of the human epithelial glycoprotein antigen EGP 314, *Oncogene* 18 (1999) 2323–2334.
- [31] J.C. Knutson, D. Yee, Electroporation: parameters affecting transfer of DNA into mammalian cells, *Anal. Biochem.* 164 (1987) 44–52.
- [32] A. Sato, S.S. Spicer, An ultrastructural and cytochemical investigation of the development of inclusions in gastric chief cells and parietal cells of mice with the Chediak-Higashi syndrome, *Lab. Invest.* 44 (1981) 288–299.
- [33] K. Kataoka, Y. Takeoka, J. Maesako, Electron microscopic observations on immature chief and parietal cells in the mouse gastric mucosa, *Arch. Histol. Jpn.* 49 (1986) 321–331.
- [34] R.J. Jackson, M.T. Howell, A. Kaminski, The novel mechanism of initiation of picornavirus RNA translation, *Trends Biochem. Sci.* 15 (1990) 477–483.
- [35] H. Komano, Y. Fujita, M. Kawaguchi, S. Matsumoto, Y. Hashimoto, S. Obana, P. Mombaerts, S. Tonegawa, H. Yamamoto, S. Itoharu, M. Nanno, H. Ishikawa, Homeostatic regulation of intestinal epithelia by intraepithelial $\gamma\delta$ T cells, *Proc. Natl. Acad. Sci. U. S. A.* 92 (1995) 6147–6151.
- [36] M. Herlyn, Z. Stepiewski, D. Herlyn, H. Koprowski, Colorectal carcinoma-specific antigen: detection by means of monoclonal antibodies, *Proc. Natl. Acad. Sci. U. S. A.* 76 (1979) 1438–1446.
- [37] J.M. Mattes, J.G. Cairncross, L.J. Old, K.O. Lloyd, Monoclonal antibodies to three widely distributed human cell surface antigen, *Hybridoma* 2 (1983) 253–264.
- [38] H. Durbin, H. Rodrigues, W.F. Bodmer, Further characterization, isolation and identification of the epithelial cell surface antigen defined by monoclonal antibody AUA1, *Int. J. Cancer* 45 (1990) 562–565.
- [39] D.P. Edwards, K.T. Grzyd, L.E. Walker, Monoclonal antibody identification and characterization of a Mr 43,000 membrane glycoprotein associated with human breast cancer, *Cancer Res.* 46 (1986) 1306–1317.
- [40] N.M. Varki, R.A. Reisfeld, L.E. Walker, Antigens associated with a human lung adenocarcinoma defined by monoclonal antibodies, *Cancer Res.* 44 (1984) 681–687.
- [41] F. Momburg, G. Moldenhauer, G.J. Hammerling, P. Moller, Immunohistochemical study of the expression of a Mr 34,000 human epithelium-specific surface glycoprotein in normal and malignant tissues, *Cancer Res.* 47 (1987) 2883–2891.
- [42] H. Haisma, H. Pinedo, A. Rijswijk, I. der Meulen-Muileman, B. Sosnowski, W. Ying, V. Beusechem, B. Tillman, W. Gerritsen, D. Curiel, Tumor-specific gene transfer via an adenoviral vector targeted to the pan-carcinoma antigen EpCAM, *Gene Ther.* 6 (1999) 1469–1474.
- [43] S. Welt, G. Ritter, Antibodies in the therapy of colon cancer, *Semin. Oncol.* 26 (1999) 683–690.
- [44] D. Herlyn, H.F. Sears, C.F. Ernst, D. Iliopoulos, Z. Stepiewski, H. Koprowski, Initial clinical evaluation of two murine IgG2a monoclonal antibodies for immunotherapy of gastrointestinal carcinoma, *Am. J. Clin. Oncol.* 14 (1991) 371–378.
- [45] S.V. Litvinov, M.P. Velders, H.A.M. Bakker, G.J. Fleuren, S.O. Warnaar, Ep-CAM: a human epithelial antigen is a homophilic cell-cell adhesion molecule, *J. Cell Biol.* 125 (1994) 437–446.
- [46] S.V. Litvinov, H.A.M. Bakker, M.M. Gourevitch, M.P. Velders, S.O. Warnaar, Evidence for a role of the epithelial glycoprotein 40 (Ep-CAM) in epithelial cell-cell adhesion, *Cell Adhesion Commun.* 2 (1994) 417–428.
- [47] M.L. Hermiston, J.I. Gordon, In vivo analysis of cadherin function in the mouse intestinal epithelium: essential roles in adhesion, maintenance of differentiation, and regulation of programmed cell death, *J. Cell Biol.* 129 (1995) 489–506.
- [48] J. Mengaud, H. Ohayon, P. Gounon, R.M. Mege, P. Cossart, E-cadherin is the receptor for internalin, a surface protein required for entry of *L. monocytogenes* into epithelial cells, *Cell* 84 (1996) 923–932.
- [49] M. Balzar, H.A.M. Bakker, I.H. Briaire-deBruijn, G.J. Fleuren, S.O. Warnaar, S.V. Litvinov, Cytoplasmic tail regulates the intracellular adhesion function of the epithelial cell adhesion molecule, *Mol. Cell Biol.* 18 (1998) 4833–4843.
- [50] M. Balzar, M.J. Winter, C.J. de Boer, S.V. Litvinov, The biology of the 17-1A antigen (Ep-CAM), *J. Mol. Med.* 77 (1999) 699–712.
- [51] M.J. Winter, I.D. Nagtegaal, J.H.J.M. van Krieken, S.V. Litvinov, The epithelial cell adhesion molecule (Ep-CAM) as a morphoregulatory molecule is a tool in surgical pathology, *Am. J. Pathol.* 163 (2003) 2139–2148.
- [52] L. Lefrancois, B. Fuller, J.W. Huleatt, S. Olson, L. Puddington, On the front lines: intraepithelial lymphocytes as primary effectors of intestinal immunity, *Springer Semin. Immunopathol.* 18 (1997) 463–475.
- [53] K.L. Cepek, S.K. Shaw, C.M. Parker, G.J. Russell, J.S. Morrow, D.L. Rimm, M.B. Brenner, Adhesion between epithelial cells and T lymphocytes mediated by E-cadherin and the $\alpha\text{E}\beta_7$ integrin, *Nature* 372 (1994) 190–193.
- [54] P. Karella, S. Bowden, S. Green, P. Kilshaw, Recognition of E-cadherin on epithelial cells by the mucosal T cell integrin $\alpha\text{M}290\beta_7$ ($\alpha\text{E}\beta_7$), *Eur. J. Immunol.* 25 (1995) 852–856.
- [55] J.M.G. Higgins, D.A. Mandelbrot, S.K. Shaw, G.J. Russell, E.A. Murphy, Y.T. Chen, W.J. Nelson, C.M. Parker, M.B. Brenner, Direct and regulated interaction of integrin $\alpha\text{E}\beta_7$ with E-cadherin, *J. Cell Biol.* 140 (1998) 197–210.
- [56] M.P. Schon, A. Arya, E.A. Murphy, C.M. Adams, U.G. Strauch, W.W. Agace, J. Marsal, J.P. Donohue, H. Her, D.R. Beier, S. Olson, L. Lefrancois, M.B. Brenner, M.J. Grusby, C.M. Parker, Mucosal T lymphocyte numbers are selectively reduced in integrin αE (CD103)-deficient mice, *J. Immunol.* 162 (1999) 6641–6649.
- [57] A.J. Nelson, R.J. Dunn, R. Peach, A. Aruffo, A.G. Farr, The murin homolog of human Ep-CAM, a homotypic adhesion molecule, is expressed by thymocytes and thymic epithelial cells, *Eur. J. Immunol.* 26 (1996) 401–408.

Therapeutic Effects of a New Lymphocyte Homing Reagent FTY720 in Interleukin-10 Gene-deficient Mice with Colitis

Tsunekazu Mizushima, MD,* Toshinori Ito, MD, PhD,* Daisuke Kishi, MD, PhD,* Yasuyuki Kai, MD,† Hiroshi Tamagawa, MD, PhD,* Riichiro Nezu, MD, PhD,† Hiroshi Kiyono, DDS, PhD,‡ and Hikaru Matsuda, MD, PhD*

Background: FTY720 is a novel reagent that possesses potent immunosuppressive activity. The immunosuppression induced by FTY720 is mediated by completely different mechanisms from those of conventional immunosuppressants, that is, by altering the tissue distribution of lymphocytes rather than inhibiting activation. In this study, we examined the efficacy of FTY720 in the treatment of chronic colitis in an interleukin-10 gene-deficient (IL-10^{-/-}) mouse model.

Methods: FTY720 was administered orally for 4 weeks to IL-10^{-/-} mice with clinical signs of colitis. The gross and histologic appearance of the colon and the numbers, phenotype, cytokine production, and apoptosis of lymphocytes were compared with those characteristics in a control group.

Results: Single-dose administration of FTY720 resulted in the sequestration of circulating lymphocytes within the secondary lymphoid tissues. Four-week administration resulted in a significant reduction of the CD4⁺ T lymphocytes subpopulation in the colonic lamina propria and IFN- γ production of the colonic lymphocytes, accompanied by a significant decrease in the severity of colitis.

Conclusions: Treatment of established colitis in IL-10^{-/-} mice with FTY720 ameliorated the colitis, probably as a result of decreasing the number of lymphocytes in the colonic mucosa and an associated reduction in IFN- γ production.

Key Words: FTY720, inflammatory bowel disease, interleukin-10 gene-deficient mice, lymphocyte homing

(*Inflamm Bowel Dis* 2004;10:182–192)

Crohn's disease is a chronic inflammatory bowel disease (IBD) of the human gastrointestinal tract. The pathogenesis of Crohn's disease remains undefined, but may involve

multiple interactions between genetic factors and environmental triggers. Likely, Crohn's disease is mediated by T lymphocytes, which arise in genetically susceptible persons as a result of dysregulation of mucosal immune responses.^{1–3} Five-amino salicylic acid (5-ASA) and corticosteroids are traditionally used as medical therapy for IBD.^{4–7} Newer therapies are aimed at delivering the active components of these agents to the diseased sites, reduction or suppression of some enteric flora, or modulation of focal immunologic targets.^{8–11} Monoclonal antibody (mAb) therapy against inflammatory mediators, such as TNF- α and IL-6 (infliximab, MRA), and leukocyte and granulocyte apheresis have recently been successful in the treatment of acute-phase IBD.^{12–17} However, current medical therapy for IBD, especially for maintenance of remission, is not ideal, and new approaches are needed.

The new synthetic immunosuppressive reagent, FTY720 (2-amino-2- [2-(4-octyl-phenyl) ethyl]-1,3-propanediol hydrochloride), is a derivative of ISP-1 (myriocin) isolated from the fungus *Isaria sinclairi*. Unlike cyclosporine, tacrolimus, and corticosteroids, FTY720 neither inhibits T lymphocyte activation and proliferation nor induces a generalized immunosuppressive status. Thus, granulocytes, monocytes, and T and B lymphocyte memory responses are unimpaired. This feature of FTY720 may provide it a distinct advantage over current immunosuppressive therapy. In recently reported studies, the administration of a single oral dose of FTY720 induced a rapid and marked reduction of peripheral blood (PB) lymphocytes^{18–20}; FTY720 shifted the distribution of lymphocytes from PB and spleen (SP) to secondary lymphoid tissues, such as Peyer's patches (PP), peripheral lymph nodes, and mesenteric lymph nodes (MLN).^{18,19} This cell redistribution by FTY720 has been attributed to a chemokine-dependent effect on lymphocyte homing.²¹ Because the immunosuppressive mechanism of FTY720 differs markedly from that of currently used immunosuppressive agents, the agent may be a promising new approach to the treatment of immunopathologic disorders, such as autoimmune diseases, and of organ transplant rejection.

In interleukin-10 gene-deficient (IL-10^{-/-}) mice, a Crohn's-like colitis develops when the mice are bred under conventional animal-care conditions but not under germ-free

Received for publication May 9, 2003; accepted September 10, 2003.

From the *Department of Surgery (E1), Osaka University Graduate School of Medicine; †Department of Surgery, Osaka Rosai Hospital; and ‡Division of Mucosal Immunology, Department of Microbiology and Immunology, The Institute of Medical Science, The University of Tokyo, Japan.

Reprints: Toshinori Ito, MD, PhD, Department of Surgery (E1), Osaka University Graduate School of Medicine, 2-2 E1 Yamadaoka, Suita City, Osaka, 565-0871 (e-mail: juki@surg1.med.osaka-u.ac.jp).

Copyright © 2004 by Lippincott Williams & Wilkins

conditions.²² Colitis in IL-10^{-/-} mice is characterized by infiltration of activated CD4⁺ T lymphocytes and macrophages into the intestinal lamina propria.²³ We hypothesize that the administration of FTY720 will deplete peripheral lymphocytes by promoting sequestration of lymphocytes in the secondary lymphoid tissues and thereby reducing the homing of lymphocytes into the lamina propria and ameliorating the chronic colitis. The current study was performed to test this hypothesis.

MATERIALS AND METHODS

Mice

Breeding pairs of IL-10^{-/-} mice on a C57BL/6 background were purchased from Jackson Laboratory (Bar Harbor, ME). C57BL/6 mice (wild type: WT) were purchased from Japan CLEA (Tokyo, Japan). Before use, the mice were maintained in a specific pathogen-free animal facility at the Institute of Experimental Animal Sciences, Osaka University Graduate School of Medicine. Mice of both genders, aged 16–20 weeks, were used. Preliminary experiments demonstrated that, under standard laboratory conditions, IL-10^{-/-} mice developed a progressive colitis from 4 weeks of age. Clinical manifestations of the disease included the passage of mucus in the stools, diarrhea, rectal prolapse, and weight loss of >5% of total body weight.

Drug Treatment of Mice

FTY720 (Novartis Pharma AG, Basel, Switzerland) was dissolved in sterile distilled water. For *in vivo* treatment, the drug was administered by gavage at a dose of 0.3 mg/kg⁻¹/day⁻¹ to 16–20-week-old IL-10^{-/-} mice that had clinical signs of colitis. Control mice received distilled water alone. At weekly intervals, the general condition and the body weight of each mouse were recorded. Mice were killed by deep anesthesia with pentobarbital sodium at the indicated time points. In the first experiments, mice were killed at 12 hours after an oral administration of FTY720. The numbers, phenotypes, and cytokine production of FTY720-treated and untreated control mice were examined. In the second experiments, mice were killed after daily administration of FTY720 for four weeks.

Isolation of Lymphoid Cells from Peripheral Blood, Spleen, and Mucosa-associated Tissues

Lymphocytes were isolated from PB, using density-separation medium (Ficoll-Paque Plus, Pharmacia Biotech AB, Uppsala, Sweden). The SP and MLN were aseptically removed, and single-cell suspensions were prepared by use of a standard mechanical disruption procedure. All MLN were taken along the ileocecal artery, and all PP were removed from whole small intestine (five to seven patches per mouse). Single-cell suspensions of PP and colonic lamina propria (CLP) lymphocytes were prepared by an enzymatic dissociation method, using collagenase as described.^{24–26}

Flow Cytometric Analysis

Immunofluorescent analysis was performed, using FACScan flow cytometry (Becton Dickinson, Mountain View, CA). Cells stained with single-color reagent were used to set the appropriate compensation levels, and at least 10,000 events were analyzed. The following mAb from BD PharMingen (San Diego, CA) were used: anti-CD4 (clone RM4-5), anti-CD8 (53-6.7), anti-CD3 ϵ (145-2C11), anti-CD45R/B220 (RA3-6B2). For two-color flow cytometry, 1 \times 10⁶ cells in 20 μ L PBS containing 2% FCS and 0.02% sodium azide were first incubated with anti-Fc receptor mAb (PharMingen, San Diego, CA) to prevent nonspecific staining and then stained with appropriate fluorescein isothiocyanate-conjugated mAb and phycoerythrin-conjugated mAb. All mAbs were used at the saturating concentrations recommended by the manufacturer. Negative control samples were stained with irrelevant, rat isotype IgG1 antibody in parallel with the experimental samples. We sought evidence that the administration of FTY720 affected the ratios of CD3⁺/B220⁺ and CD4⁺/CD8⁺ in various lymphoid-organ compartments.

Culture Conditions for the Analysis of Cytokine Production

CLP and SP lymphocytes from FTY720 treated and control mice were cultured in medium consisting of RPMI 1640 supplemented with 3 mM L-glutamine, 10 mM Hepes buffer, 10 μ g/mL gentamicin, 100 U/mL penicillin and streptomycin, 0.05 mM 2-ME, and 10% FCS (Hyclone Co., Salt Lake, UT). To measure cytokine production, CLP and SP lymphocytes (1 \times 10⁶ cell/mL), purified as described above, were loaded into wells coated with murine anti-CD3 ϵ antibody (clone 145-2C11; PharMingen, San Diego, CA) and 1 μ g/mL soluble anti-CD28 (clone 37.51; PharMingen) (to activate fully T lymphocytes, anti-CD28 antibody was used as a major costimulation together with anti-CD3 ϵ) and cultured for 48 hours. The culture supernatants were then harvested and assayed by ELISA for their cytokine concentration. For this assay, we used 24-well Costar plates (Costar Corp., Cambridge, MA), which we coated with anti-CD3 ϵ antibody by exposing the wells to a solution containing anti-CD3 ϵ antibody (10 μ g/mL) in carbonate buffer (pH 9.6) overnight at 4°C.

ELISA

IFN- γ and IL-4 concentrations were measured by use of commercially available specific ELISA assays, using duopaired murine cytokines according to the manufacturer's recommendations (PharMingen, San Diego, CA) on Immulon-4, 96-well microtiter plates (Nalge Nunc International, Rochester, NY). Optical densities were measured on a Dynatech MR 5000 ELISA reader at a wavelength of 450 nm.

Histologic Analysis of the Colon

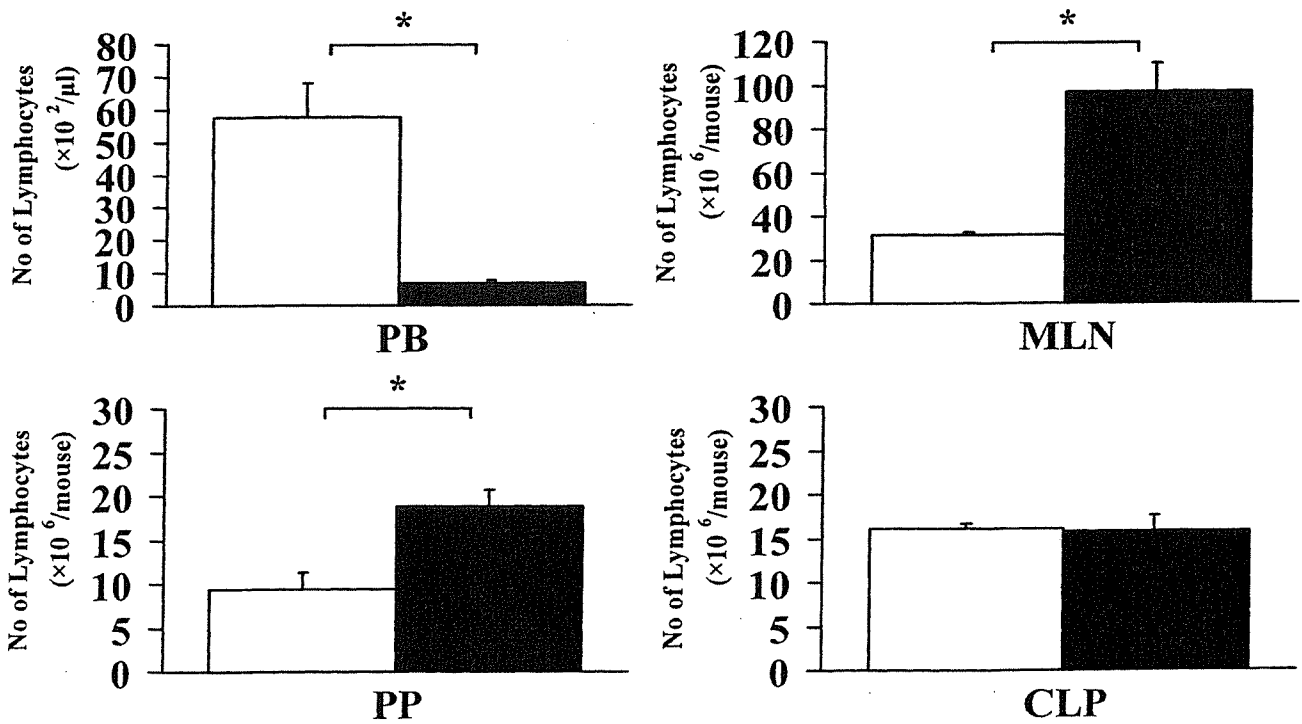
The colon was divided into three portions: proximal, middle, and distal. The tissue was fixed in 4% paraformaldehyde.

TABLE 1. The Numbers of CD3⁺, B220⁺, CD4⁺, and CD8 Lymphocytes Isolated from PB and CLP in Adult IL-10^{-/-} Mice and WT

Phenotype of Lymphocytes	PB ($\times 10^2/\mu\text{L}$)		CLP ($\times 10^6/\text{Mouse}$)	
	WT	IL-10 ^{-/-}	WT	IL-10 ^{-/-}
CD3 ⁺	8.78 \pm 2.62	23.35 \pm 3.66*	10.40 \pm 0.28	72.33 \pm 6.07*
B220 ⁺	25.63 \pm 5.39	26.43 \pm 5.78	19.43 \pm 1.94	66.66 \pm 3.89*
CD4 ⁺	6.13 \pm 1.92	13.49 \pm 2.26*	5.65 \pm 0.49	56.39 \pm 5.10*
CD8 ⁺	1.65 \pm 0.40	8.91 \pm 1.76*	4.16 \pm 0.53	15.54 \pm 0.75*

The numbers of CD3⁺, CD4⁺, and CD8⁺ lymphocytes from PB, and the numbers of B220⁺ lymphocytes as well as CD3⁺, CD4⁺, and CD8⁺ lymphocytes from CLP were significantly increased in IL-10^{-/-} mice. The data represent the values (mean \pm SEM) from three different experiments (7 mice per group). WT, wild-type; PB, peripheral blood; CLP, colonic lamina propria.

**p* < 0.05 versus WT.



□ : Control (n=5) ■ : FTY720 (n=5) Mean \pm SEM *: *p* < 0.05 vs. Control

FIGURE 1. The numbers of lymphocytes in PB, MLN, PP, and CLP after a single administration of FTY720. Mice were killed after a single administration of FTY720, and the numbers of lymphocytes in PB, MLN, PP, and CLP were examined. The numbers of PB lymphocytes were significantly decreased, whereas the numbers of MLN and PP lymphocytes were significantly increased, in IL-10^{-/-} mice treated with FTY720 (■) compared with corresponding values in untreated control mice (□). There was no significant difference in the numbers of lymphocytes in the CLP between the two groups. The data represent the values (mean \pm SEM) from three different experiments (5 mice per group).

TABLE 2. Flow Cytometric Analysis in Lymphocytes From PB, MLN, PP, and CLP of Mice Treated With a Single Dose of FTY720 and Control Mice

Lymphocytes	CD3 ⁺ /B220 ⁺ Ratios		CD4 ⁺ /CD8 ⁺ Ratios	
	Control	FTY720	Control	FTY720
PB	0.80 ± 0.17	1.18 ± 0.09	1.68 ± 0.32	1.14 ± 0.34
MLN	2.14 ± 0.19	1.48 ± 0.29	1.11 ± 0.19	1.26 ± 0.08
PP	0.24 ± 0.02	0.30 ± 0.00	3.00 ± 0.10	2.72 ± 0.64
CLP	1.22 ± 0.17	1.92 ± 0.35	4.06 ± 0.54	3.40 ± 0.51

There was no significant difference in CD3⁺/B220⁺ and CD4⁺/CD8⁺ ratios in lymphocytes from PB, MLN, PP, and CLP of mice treated with a single dose of FTY720 and control mice. The CD3⁺/B220⁺ and CD4⁺/CD8⁺ ratios in lymphocytes are expressed as the values (mean ± SEM) from three different experiments (5 mice per group). PB, peripheral blood; MLN, mesenteric lymph nodes; PP, Peyer's patches; CLP, colonic lamina propria.

hyde in PBS for 4 hours and embedded in paraffin. Two-micrometer-thick sections were cut and stained with hematoxylin and eosin.

Histopathologic alterations in the colonic mucosa were semi-quantified according to a modified scoring system: (a) cellular infiltration in the lamina propria (score from 0 to 3); (b) mucin depletion (score from 0 to 2); (c) crypt abscesses (score from 0 to 2); (d) epithelial erosion (score from 0 to 2); (e) hyperemia (score from 0 to 3); (f) thickness of the mucosa (score from 1 to 3).²⁷ Hence, the range of histopathologic score of each specimen was from 1 (no alteration) to 15 (most severe colitis) and that of each mouse was from 3 to 45.

Analysis of Lymphocyte Apoptosis

Furthermore, the degree of lymphocytes apoptosis was compared between FTY720-treated and untreated control mice. After a single or 3 days' administration of FTY720, TUNEL assay using Apop Taq Plus Kit (Oncor, Gaithersburg, MD) for terminal deoxynucleotidyl transferase-mediated dUTP nick-end labeling (TUNEL) to detect DNA fragmentation was performed. Cryosections (5 µm) of MLN and PP were fixed in 1% paraformaldehyde in a coplin jar. The sections

were quenched in 3% hydrogen peroxide in PBS for 5 minutes at room temperature and incubated at 37°C for 1 hours with deoxynucleotidyl transferase (TdT) and digoxigenin (DIG)-conjugated dUTP in reaction buffer. The reaction was terminated with a prewarmed working strength stop/wash buffer for 30 minutes at 37°C. To visualize the incorporated dUTP, the sections were incubated with peroxidase-conjugated anti-DIG antibody for 30 minutes at room temperature, then washed three times and further incubated with 3,3-diaminobenzidine (DAB) substrate working solution for 3-6 minutes at room temperature. The sections were counterstained with hematoxylin and mounted. Thus, apoptotic cells in PB, MLN, PP, and CLP were determined, using FACScan flow cytometry (Becton Dickinson, Mountain View, CA), by staining with annexin V and propidium iodide using the Annexin V FITC Apoptosis Detection Kit (BD PharMingen, San Diego, CA), according to the manufacturer's instructions.

Statistical Analysis

Statistical analysis was conducted by use of Student *t* test and the program Statview. *p* values of 0.05 were considered statistically significant.

TABLE 3. Cytokine Production by Splenocytes and CLP Lymphocytes After a Single Administration of FTY720

Lymphocytes	IFN-γ (pg/mL)		IL-4 (pg/mL)	
	Control	FTY720	Control	FTY720
SP	1500 ± 768	3930 ± 2270	15.2 ± 5.10	22.2 ± 11.8
CLP	26000 ± 3380	33300 ± 9370	7.74 ± 1.93	16.1 ± 5.27

IFN-γ and IL-4 production by splenocytes and CLP lymphocytes obtained after a single administration of FTY720 or distilled water were measured. There was no significant difference in values between the treated and control groups. The data represent the values (mean ± SEM) from three different experiments (5 mice for FTY720 treatment and 4 mice for control). SP, spleen; CLP, colonic lamina propria; IFN, interferon; IL, interleukin.

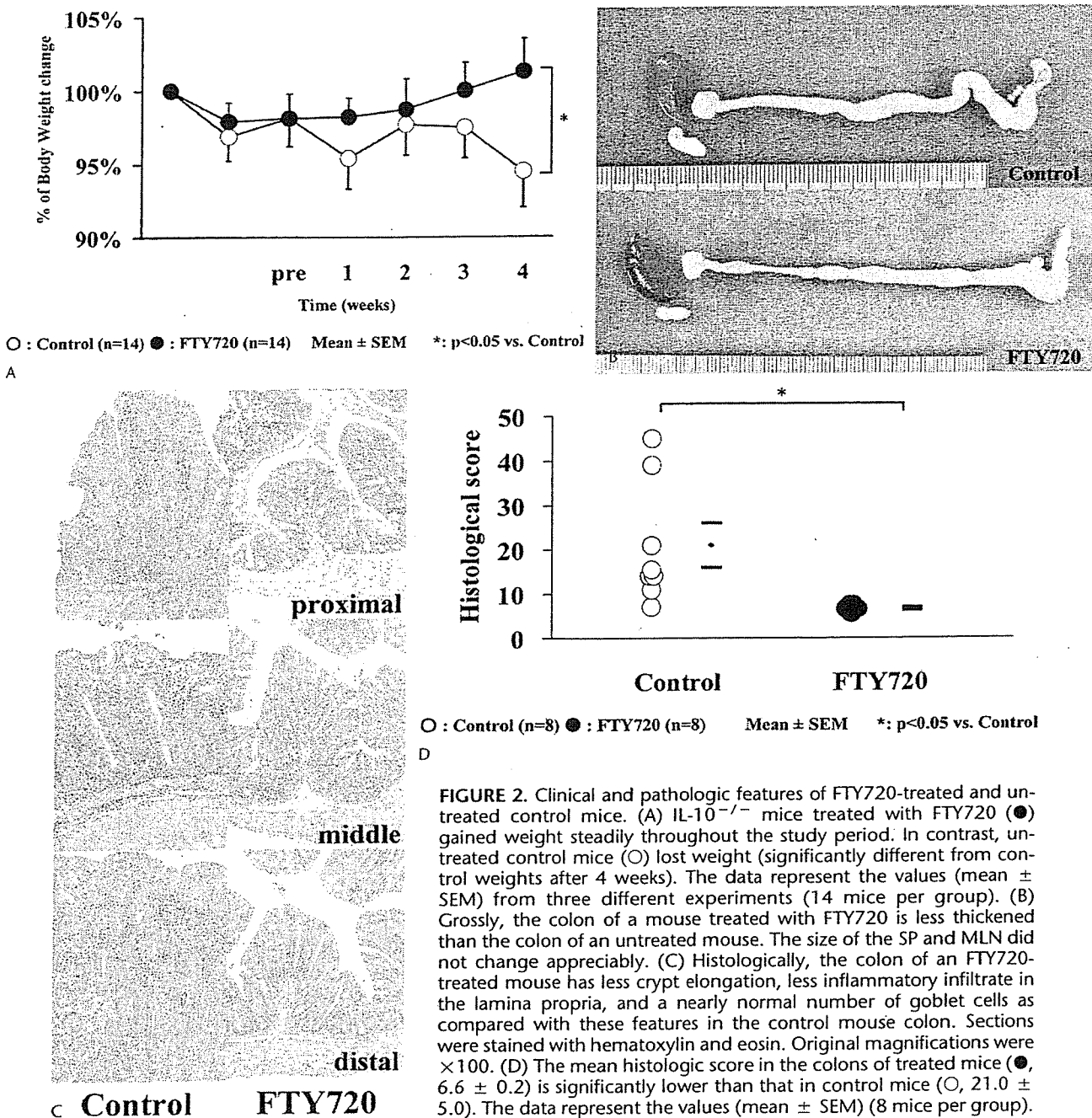


FIGURE 2. Clinical and pathologic features of FTY720-treated and untreated control mice. (A) IL-10^{-/-} mice treated with FTY720 (●) gained weight steadily throughout the study period. In contrast, untreated control mice (○) lost weight (significantly different from control weights after 4 weeks). The data represent the values (mean ± SEM) from three different experiments (14 mice per group). (B) Grossly, the colon of a mouse treated with FTY720 is less thickened than the colon of an untreated mouse. The size of the SP and MLN did not change appreciably. (C) Histologically, the colon of an FTY720-treated mouse has less crypt elongation, less inflammatory infiltrate in the lamina propria, and a nearly normal number of goblet cells as compared with these features in the control mouse colon. Sections were stained with hematoxylin and eosin. Original magnifications were ×100. (D) The mean histologic score in the colons of treated mice (●, 6.6 ± 0.2) is significantly lower than that in control mice (○, 21.0 ± 5.0). The data represent the values (mean ± SEM) (8 mice per group).

RESULTS

T Lymphocytes from PB and CLP Were Increased in IL-10^{-/-} Mice Compared with WT Mice

Flow cytometric analyses of PB and CLP lymphocytes from the IL-10^{-/-} and WT mice showed that CD3⁺,

CD4⁺, and CD8⁺ subpopulations were increased in PB lymphocytes, and B220⁺ as well as CD3⁺, CD4⁺, and CD8 subpopulations were increased in CLP lymphocytes from IL-10^{-/-} mice compared with corresponding values in the WT mice (Table 1).

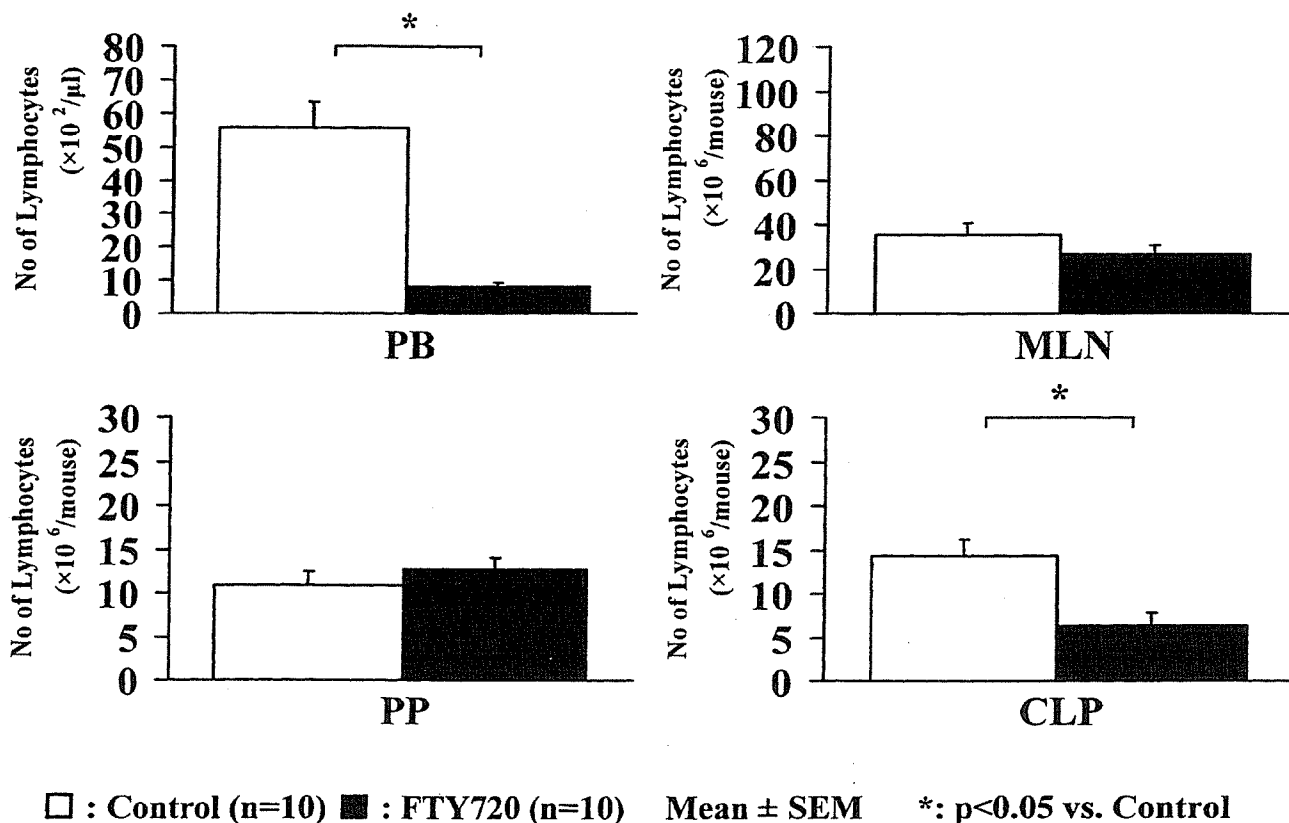


FIGURE 3. The numbers of lymphocytes in PB, MLN, PP, and CLP after 4 weeks' treatment with FTY720. Mice were killed after the daily administration of FTY720 for 4 weeks, and the lymphocytes in PB, MLN, PP, and CLP were enumerated. In comparison with lymphocyte numbers after a single-dose treatment (Fig. 1), the numbers of PBL remained significantly decreased, whereas the numbers of MLN and PP lymphocytes had returned to control values, the numbers of lymphocytes in the CLP had significantly decreased as compared with control values. The data represent the values (mean \pm SEM) from three different experiments (10 mice per group). Closed (■) and open (□) bars represent FTY720-treated and untreated control groups, respectively.

A Single Administration of FTY720 Decreased the Number of Lymphocytes in PB and Increased the Number in MLN and PP, but Did Neither Change the Phenotype nor Cytokine Production

A single administration of FTY720 significantly decreased the number of PBL in IL-10^{-/-} mice compared with that in control mice. In contrast, the numbers of lymphocytes in MLN and PP were significantly increased. The number of lymphocytes in the CLP was not changed (Fig. 1).

In lymphocytes from PB, MLN, PP, and CLP, the ratios of both CD3⁺/B220⁺ and CD4⁺/CD8⁺ showed no significant difference between mice treated with FTY720 and untreated control mice (Table 2).

There was also no significant difference in IFN- γ and IL-4 production by splenocytes and CLP lymphocytes between FTY720-treated and untreated control mice (Table 3).

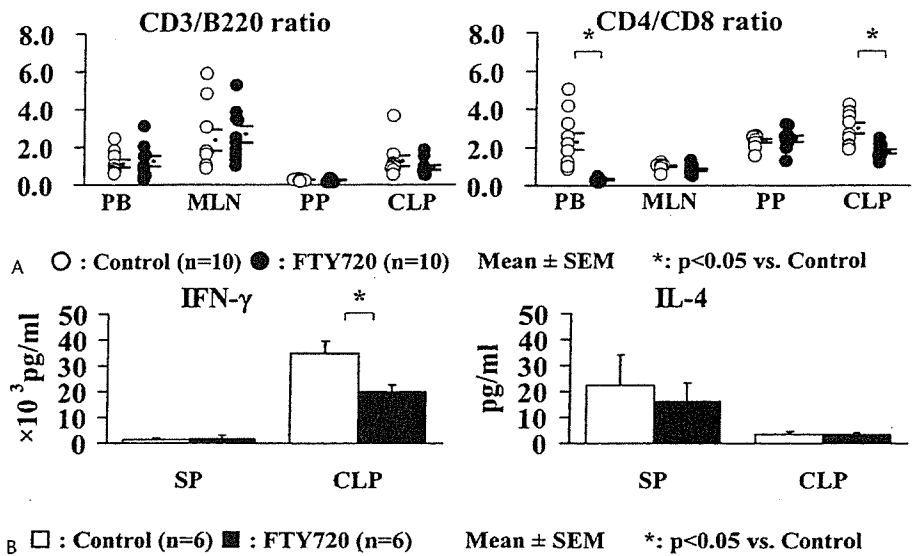
FTY720 Treatment of 4 Weeks Resulted in a Significantly Reduced Severity of Colitis

Control IL-10^{-/-} mice developed the changes of the wasting syndrome: weight loss and hunched posture. Mice treated with FTY720, however, remained in good condition and gained weight steadily (Fig. 2A). Although rectal prolapse did not change, diarrhea had been improved in some mice from around 10 days after FTY720 treatment. After 4 weeks, all mice treated with FTY720 had no diarrhea.

Macroscopically, the colonic wall in the mice treated with FTY720 was less thickened than in the untreated control mice (Fig. 2B). The size of spleens and MLN were not significantly changed.

Histologically, the intestinal lamina propria of mice treated with FTY720 had less elongation of gland crypts and much less infiltration of inflammatory cells than was present in the control mice. Also, the number of goblet cells was almost

FIGURE 4. The phenotype of lymphocytes in PB, MLN, PP, and CLP and the cytokine production by splenocytes and CLP lymphocytes. (A). The ratios of CD3⁺/B220⁺ and CD4⁺/CD8⁺ lymphocytes, determined by flow cytometric analysis, after the daily administration of FTY720 for 4 weeks. There are no differences in the ratios of either CD3⁺/B220⁺ or CD4⁺/CD8⁺ lymphocytes from MLN and PP in the treated compared with untreated control animals. In contrast, the CD4⁺/CD8⁺ ratio in lymphocytes from PB and CLP is significantly decreased. The lymphocyte ratios are expressed as the mean values from three different experiments (10 mice per group). Closed (●) and open (○) circles represent FTY720-treated and untreated control mice, respectively. (B) IFN- γ and IL-4 production by splenocytes and CLP lymphocytes after the daily administration of FTY720 for 4 weeks. There is no significant difference in the production of either cytokine by SP, or of IL-4 by CLP lymphocytes. However, IFN- γ production by CLP lymphocytes is significantly diminished. The data represent the values (mean \pm SEM) from three different experiments (10 mice per group). Closed (■) and open (□) bars represent FTY720-treated and untreated control groups, respectively.



normal in the colons of mice treated with FTY720 but reduced in those of control mice (Fig. 2C).

The mean histologic score of 16–20-week-old IL-10^{-/-} mice just before starting treatment was 15.5 \pm 1.7 in our animal facility. After 4 weeks, the histologic scores of mice treated with FTY720 were significantly decreased as compared with those of control mice (Fig. 2D: 6.6 \pm 0.2 vs 21.0 \pm 5.0).

Daily Administration of FTY720 for 4 Weeks Significantly Decreased the Number of Lymphocytes in CLP

After four weeks’ treatment with FTY720, the number of lymphocytes in PB was still significantly lower than that in control animals. The numbers of lymphocytes in MLN and PP had returned to the control level. Most interestingly, the number of lymphocytes in the CLP had significantly declined compared with control values (Fig. 3).

Daily Administration of FTY720 for 4 Weeks Significantly Decreased the Numbers of CD4⁺ Lymphocytes in PB and CLP

Flow cytometric analysis performed on lymphocytes collected after 4 weeks of treatment revealed that the ratios of both CD3⁺/B220⁺ and CD4⁺/CD8⁺ in lymphocytes from MLN and PP were not significantly different from corresponding values in control mice. In contrast, the CD4⁺/CD8⁺ ratio in

lymphocytes from PB and CLP was significantly reduced (Fig. 4A).

Daily Administration of FTY720 for 4 Weeks Resulted in Decreased Production of IFN- γ by CLP Lymphocytes

After 4 weeks’ treatment with FTY720, there was no significant difference in IFN- γ and IL-4 production by splenocytes or in IL-4 production by CLP lymphocytes. However, IFN- γ production by CLP was significantly diminished (Fig. 4B).

Apoptotic Lymphocytes Were Detected in MLN and PP, but Were Not Enhanced by FTY720 Treatment

After a single or 3 days’ administration of FTY720, we could detect quite a number of TUNEL positive cells in MLN and PP, but no significant difference was observed between FTY720-treated and untreated control mice (Fig. 5A).

There was no significant difference in the percentage of annexin-positive/propidium iodide-negative lymphocytes from PB, MLN, PP, and CLP of mice treated with a single dose of FTY720 and untreated control mice (Fig. 5B).

DISCUSSION

The chronic gastrointestinal inflammation in Crohn’s disease and various experimental models of colitis is associ-

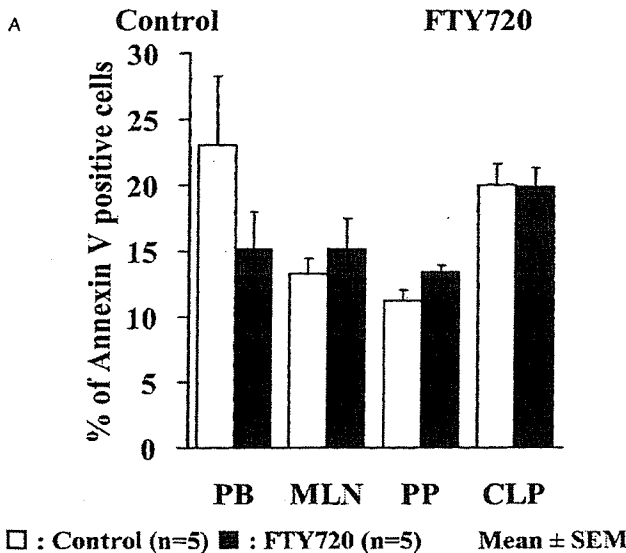


FIGURE 5. The degree of lymphocyte apoptosis after FTY720 treatment. (A) TUNEL assay of the MLN and PP from IL-10^{-/-} mice treated with FTY720 and untreated control mice. After 3 days' administration of FTY720, quite a number of TUNEL positive cells were detected in MLN and PP of an FTY720-treated mouse, but were not significantly different from those of control mice. Original magnifications were ×100. B; The percentage of lymphocyte apoptosis after a single administration of FTY720. There was no significant difference in the percentage of annexin-positive/propidium iodide-negative lymphocytes from PB, MLN, PP, and CLP of mice treated with a single dose of FTY720 and control mice. The data represent the values (mean ± SEM) from three different experiments (5 mice per group).

ated with a breakdown of oral tolerance to some food antigens and resident enteric bacteria. This breakdown results in T-cell activation and the production of chemokines, proinflammatory monokines and T_H1 cytokines.^{1-3,28} IL-10^{-/-} mice spontane-

ously develop enterocolitis by 2-3 months of age, with multifocal inflammatory lesions throughout the gastrointestinal tract²² that have similarities to human Crohn's disease. The chronic colitis in IL-10^{-/-} mice is mediated by CD4⁺ T_H1 cells exclusively producing IFN-γ.^{29,30} Transfer of specific colonic T-cell subsets from IL-10^{-/-} mice into RAG-2^{-/-} (lymphocyte-depleted) mice has produced a colitis like that in IL-10^{-/-} mice.²⁹ In the current study, we confirmed the report of Berg et al³¹ that CD3⁺, CD4⁺, and CD8⁺ subpopulations of PB and CLP lymphocytes are markedly increased in IL-10^{-/-} mice as compared with WT mice. We suspect that the pathogenesis of colitis in IL-10^{-/-} mice is due to defects in mechanisms regulating the continuous activation of lymphocytes, homing of activated PB lymphocytes into CLP, and the production of inflammatory cytokines in the colon.

There have been many trials of inhibiting various cytokines in IL-10^{-/-} mice in attempts to prevent the development of colitis or to treat established colitis.²⁹⁻³² Administration of anti-IFN-γ mAb, anti-IL-12 mAb or IL-10 to young IL-10^{-/-} mice has significantly prevented the development of disease in adult mice.^{30,31} Only systemic injection of adenoviral vector encoding murine IL-10 gene-induced clinical and histologic remission in mice with established disease.³³ Thus, it appears difficult to treat established colitis by inhibiting various cytokines. Perhaps it will be necessary in this circumstance to control directly the activated CD4⁺ T lymphocytes themselves.

Immunologically mature lymphocytes continuously recirculate in the PB, spleen, lymphatic vessels, peripheral lymph nodes, and gut-associated lymphoid tissues (Fig. 6A).³⁴ This recirculation of lymphocytes (homing) is essential for the development of effective immune responses to foreign antigens. The intestinal mucosal immune system, which connects inductive (eg, PP) and effector (eg, CLP) sites, is well characterized.^{35,36} Naive T lymphocytes preferentially leave the blood stream, enter secondary lymphoid tissues, such as PP and MLN, and cross the high endothelial venules, where some of the cells interact with antigen-presenting cells. The activated T lymphocytes then return to the blood stream through the afferent lymphatic vessels and thoracic duct, leave the blood stream, and eventually enter the intestinal mucosa.³⁷ This lymphocyte homing depends on and is regulated by at least four adhesive interactions between lymphocytes and vascular cells: selectin-mediated cell rolling, activation through G protein-coupled receptors (GPCRs), integrin-mediated strong adhesion, and transendothelial migration into the tissue.^{38,39} Lymphocytes expressing integrinα4β7 are a cell population that preferentially migrates to the gut using specific interaction between integrinα4β7 and MAdCAM-1, whereas non-mucosal T lymphocytes, using the integrinα4β1/VCAM-1 system, migrate to extraintestinal lymphoid tissues. In the mucosal immune system, pathogenic lymphocytes also are activated in PP and selectively move into CLP through the inter-

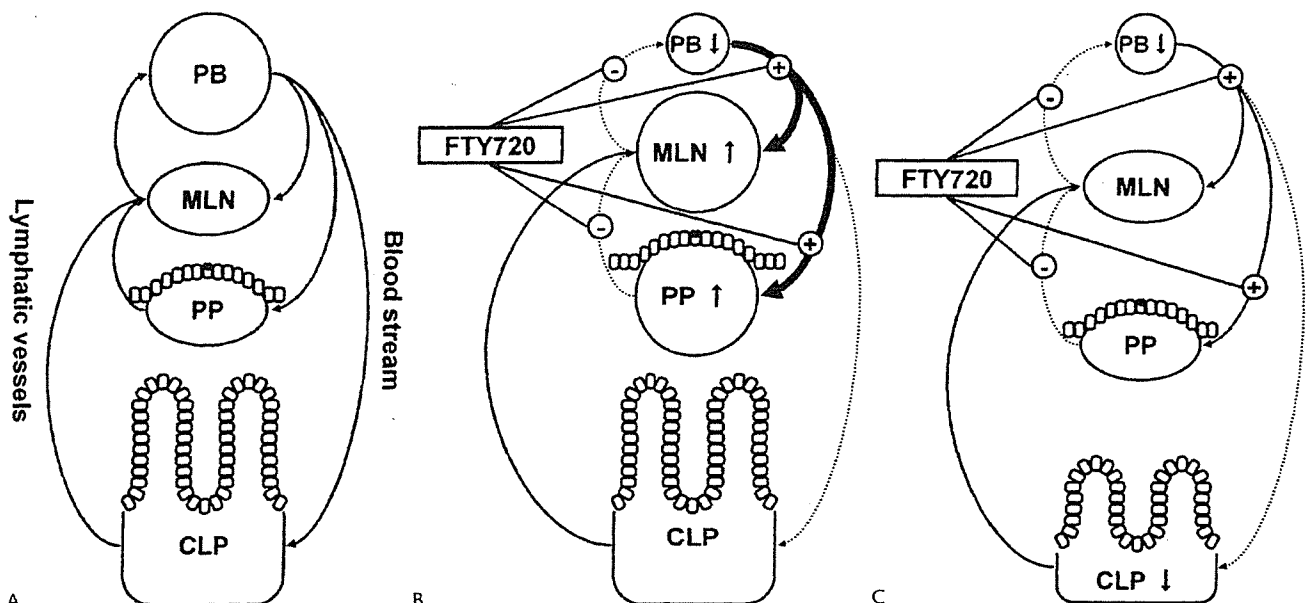


FIGURE 6. Schematic representation of our results. (A) In the intestinal mucosal immune system, immunologically mature lymphocytes continuously recirculate in the PB, lymphatic vessels, inductive (eg, PP) and effector (eg, CLP) tissues. (B) FTY720 treatment resulted in the sequestration of circulating lymphocytes from PB into MLN and PP and reduced the supply of lymphocytes migrating to the inflammatory site from the PB. (C) Continuous administration of FTY720 prevented activated lymphocytes at inductive sites, such as PP, from recirculating into the periphery, consequently resulting in a decreased infiltration of lymphocyte into the CLP.

action between integrin α 4 β 7 and MAdCAM-1.³⁸ MAbs against some adhesion molecules and their ligands have blocked these processes and ameliorated the intestinal inflammation. For example, anti- β 7 mAb treatment of scid mice reconstituted with CD45RB^{high} CD4⁺ T cells, and anti- α 4 β 7 mAb treatment of IL-2^{-/-} mice, significantly reduced the severity of colitis.^{40,41} Also, treatment with the anti- α 4 integrin mAb (natalizumab) has induced clinical remission in active Crohn's disease.⁴²

Immunosuppressive reagents, such as cyclosporine and tacrolimus, have facilitated organ transplantation, but their utility remains limited because of their toxicities, and the agents are not very effective in the chronic management of autoimmune diseases. FTY720 seems attractive because, unlike conventional immunosuppressants, it induces a lymphopenia through a reversible homing of lymphocytes from PB to secondary lymphoid tissues, such as MLN and PP, with a concomitant reduction of specific effector T cells recirculating from the lymphoid tissues to peripheral sites.⁴³⁻⁴⁵ The molecular mechanisms responsible for this lymphocyte homing are not defined, but some clues exist. Sphingosine, structurally similar to FTY720, is phosphorylated by sphingosine kinase to become sphingosine 1-phosphate (S1P). S1P has altered lymphocyte trafficking by activating S1P receptors.⁴⁶ FTY720 phosphoryl metabolites as well as S1P

are high-affinity agonists of S1P receptors and mediate their effects through 5 GPCRs (S1P receptors) on the surface of lymphocytes. Although the precise mechanisms remains unknown, these S1P receptor agonists could induce emptying of lymphoid sinuses by retention of lymphocytes on abluminal side of sinus-lining endothelium and inhibition of egress into lymphatic vessels.^{47,48} Therefore, after phosphorylation, FTY720 may act through the S1P signal pathway by activating S1P receptors to modulate chemotactic responses and lymphocyte trafficking, thereby inhibiting lymphocyte recirculation.^{47,48}

In the current work, we first evaluated the possible preventive effect of FTY720 on colitis in IL-10^{-/-} mice. The administration of the reagent for 8 weeks to 4-week-old animals, which had not yet developed colitis, completely prevented the development of colitis. Furthermore, FTY720 prevented the infiltration of lymphocytes into the CLP (data not shown). We next examined the effect of a single administration of FTY720 to IL-10^{-/-} mice with established colitis. We found the PB lymphocytes to be significantly decreased, but they returned to normal levels after a few days (Fig. 6B). Furthermore, this treatment did not produce any specific effects directly on lymphocyte subpopulations or cytokine production by the lymphocytes. These results suggested that FTY720 reduced the migration of lymphocytes from PB to the inflammatory sites. Thus,